

Response to Anonymous Referee #1

This paper presents a thorough multi-scale chemistry-transport modeling analysis of a volcanic plume from the Ambrym volcano (Vanuatu). Model simulations are evaluated against ground-based and satellite observations of SO₂ and BrO. A lot of care is put in estimating as accurately as possible model inputs, notably the mix (sulphur, halogen), vertical distribution and rates of volcanic emissions. The authors set up a complex model configuration to generate a realistic transport of volcanic emissions. In order to resolve the plume at different scales and phases, the atmospheric model domain is 3 nested grids centred over the volcano going to a resolution of 500 x 500 m; ECMWF meteorological analyses (wind, temperature, water vapour) are used to initialize and nudge the model. A range of model simulations is performed to cover the uncertainties in model inputs and chemistry (e.g. high temperature chemistry, plume height,:::

). The introduction on volcanic halogen is rather thorough. However, it does mention the issue of the transport of volcanic halogen to the stratosphere and the possible implications for stratospheric ozone. It is a bit surprising because this point pops out a few times in the manuscript. For example, it is mentioned in section 4.2.2: “Such transport of volcanic bromine to the upper troposphere and the stratosphere is of strong interest. Indeed, the stratospheric bromine burden is underestimated by global models that take only into account long lived halons and methyl bromide”. Again, in the conclusion, the authors recall an important finding in their model simulations: “There is also evidence in the simulations of a subsequent transport of bromine to the stratosphere from Ambrym”. They also state that “longer duration simulations should be performed to fully quantify the impact of Ambrym on chemical composition of the troposphere at the regional scale. In particular, flux of bromine to upper troposphere and to the stratosphere from this extreme continuous degassing event”. They never provide references and this point is not mentioned in the introduction. The references are about the impact of volcanic halogen on tropospheric chemistry. I would suggest to mention the impact of volcanic halogens on the stratosphere, notably the ozone layer, in the introduction with references. This issue has been largely overlooked in the literature. But, several recent studies have shown that volcanic halogen, notably bromine, from very large volcanic events could have had a drastic effect on the evolution of stratospheric ozone in the past, when the atmospheric chlorine and bromine loadings were low (in contrast to the present-day atmosphere). The key uncertainty in assessing the impact of volcanic halogen from massive eruptions on stratospheric ozone is the fraction of bromine and chlorine emissions reaching the stratosphere which depend on the form of the volcanic halogen injected. If bromine and chlorine are in the form of HBr and HCl (acidic molecules, soluble), they would tend to be eliminated very quickly within the plume by dissolution in aqueous phases or/and adsorption on solid particles. In contrast, bromine and chlorine radicals are much less soluble, so they would survive longer in the volcanic plume and hence are more likely to reach the stratosphere. Therefore, the process of halogen activation in volcanic plumes is highly relevant to the question of the potential impact of volcanic halogen on stratospheric ozone.

We agree with the reviewer’s comment. We have now added the impact of volcanic halogens emitted by explosive eruptions on stratospheric ozone (with the references to relevant articles) in a paragraph in the Introduction :

“On the other hand, the impact of other compounds as halides (HCl, HBr) injected by explosive eruptions into the stratosphere as well as the overall impact of minor eruptions and quiescent passive degassing have been largely overlooked. However, the presence of volcanic

halogens in the stratosphere following explosive eruptions has been recently detected (e.g., Hunton et al., 2005; Rose et al., 2006; Prata et al., 2007; Theys et al., 2014, Carn et al., 2016). Such volcanic halogen injection, enabled by incomplete volcanic halides washout as first predicted by a model study (Textor et al., 2003), was found to cause enhanced reactive chlorine and bromine as well as enhanced ozone depletion (Rose et al., 2006; Millard et al., 2006). As a result, it is important, as emphasized in Cadoux et al. (2015), to consider volcanic halogens in addition to sulfur compounds when studying the influence on the stratosphere of past and future explosive eruptions.”

We have also mentioned in the Conclusion the potential impact of halogen activation in tropospheric plumes on stratospheric ozone :

“There is also evidence in the simulations of a subsequent transport of bromine to the stratosphere from Ambrym. Thus, the halogen activation in tropospheric volcanic plumes could be one aspect of the potential impact of volcanic halogen on stratospheric ozone.”

The first part of the paper is devoted to the analysis of near field plume focusing on the higher resolution model nests. Overall, the results are encouraging. Comparisons between simulations and ground-based/satellite SO₂ observations indicate that the model performs rather well regarding the transport and dispersion of the plume. Sensitivity simulations confirms that the high temperature chemistry in the vent of the volcano is important because, by taking it into account, the model is able to reproduce the general evolution of BrO/SO₂ seen in DOAD data downwind from the vent. The main discrepancy is about the magnitude of BrO columns that the model underestimates by about a factor 3. The authors point out that the fact that BrO formation is limited by the flux of ozone in the near-downwind plume could explain some of the discrepancy. Unlike a 1-D plume model, the level of mixing between the plume and the ambient air is a factor whose influence they cannot easily explore in their 3-D model configuration. Plume chemistry and the associated changes in chemical composition strongly depend on the entrainment flux of outside air. Clearly, the different changes, notably ozone destruction and BrO formation, do not have the same dependency on the mixing rate. For instance, the lower the mixing is, the more pronounced the local ozone destruction, but the lower the formation and hence the levels of BrO are. This discrepancy may indicate that the level of mixing is not quite right yet. The balance between mixing and chemistry is difficult to strike.

We agree with the reviewer’s summary. In the section 3.3.1, we have modified the text to make it clear that through a sensitivity study on plume depth, we test the effect of plume-air mixing. We agree though that efforts to test plume-air mixing are more challenging with a full 3D model than with 1D models where the mixing is to a large extent user-tuned.

Anyway, I think the authors went as far as possible with their model configuration. Another possible cause for the discrepancy is the halogen activation scheme because there are large uncertainties pertaining to aqueous phase chemistry.

This point is now mentioned in the manuscript in the section 3.3.3. In this section, we have performed a sensitivity study where we have increased the sulfate aerosol surface density. This is equivalent to keep the aerosol surface density constant but to increase the reactive uptake coefficients of HOBr and BrONO₂. Indeed, there are a lot of uncertainties on the values of uptake coefficients as shown in Roberts et al. (2014b) where HOBr +HBr and HOBr +HCl reactive uptake coefficient have been reevaluated.

It is also important to note, as mentioned elsewhere in our responses to Reviewer 2, that the discrepancy between observed and simulated BrO columns is now better characterized in the text. We find that the model indeed underestimates by 60% in average the magnitude of observed BrO columns in the closest transect at 15 km from the vents. But, the model is in much better agreement with the DOAS observations made in the furthest transect (~40 km from the vents). In this case, the mean difference between observation and model is only 14%. Overall, we find that the model underestimates the BrO DOAS observations by 40 % in average. We have now made clear as well that this bias does not significantly impact our regional impact analysis as it has already decreased to 14 % at 40 km.

The second part of the paper is devoted to the analysis of far field plume focusing on the large-scale model domain where the resolution is 50x50 km. Large-scale model simulations are evaluated against SO₂ columns. It is a pity that simultaneous BrO observations are not available. The authors discuss the model-calculated impact on the lifetimes and budget of several trace gases (e.g. ozone, methane, OH, SO₂). All the results confirm that volcanic halogen emissions may play a significant role in atmospheric chemistry, at least on a regional scale.

In conclusion, I congratulate the authors for this solid piece of multi-scale volcanic plume modelling. This work is a big step forward from the simple 1-D plume approach. It allows a more critical testing of model simulations against observations because the transport and dispersion of the plume are much better constrained.

The model results confirm the potential importance of volcanic halogen on the budget of a range of trace gases. The magma of some volcano is extremely rich in halogen. Therefore, when assessing their impact on atmospheric composition and climate, the halogen component should be not neglected. I recommend publication. However, it might be good for the authors to take on board some of my comments and suggestions listed above.

Response to Anonymous Referee #2

With the aim of studying the sulfur- and halogen-rich emissions of Ambrym volcano (Vanuatu), the authors have included volcanic reactive halogen chemistry in a chemistry-transport model. This is an important effort and step forward in the study of volcanic reactive halogen chemistry, which has been restricted so far to 1-D chemistry models essentially. Ambrym volcano is a well-chosen case-study as it represents one of the most important source of persistent volcanic degassing on Earth, with substantial bromine emissions. This makes Ambrym an appropriate target for a first 3D modeling attempt. On the other hand, volcanic BrO observations are still sparse as BrO abundance is most often below satellite detection and consequently requires ground-based measurements to be evaluated. Regarding Ambrym volcano, ground-based observations of both sulfur dioxide (SO₂) and bromine oxide (BrO) column amounts, at various distances downwind from the crater are available making this volcano a good candidate.

This paper starts with an analysis of the BrO formation process, leading the authors to confirm previous findings achieved by 1D-models : they highlight the importance of model initialisation with high-temperature chemistry at the vent ; they also recognize that the highest SO₂/BrO values are located at the edge of the plume because of

enhanced mixing with ozone-rich background air.

In the following part, the authors attempt a comparison of their model outputs against observations, with the aim of fitting the measured SO₂ and BrO abundances. Model outputs show a large underestimation of predicted BrO abundance by a factor of about 3.

The reviewer's comments helped us understand that the 'factor 3' discrepancy between model and DOAS observations for BrO columns was too much over-emphasized in our original manuscript. Indeed this factor refers to the ratio between the maximal DOAS BrO columns measured in the near downwind (~ 15 km from the vents) plume and its modeled counterpart. The model indeed underestimates by 60% in average the magnitude of observed BrO columns in the closest transect at 15 km from the vents. But, the model is in much better agreement with the DOAS observations made in the furthest transect (~40 km from the vents). In this case, the mean difference between observation and model is only 14% (relative to the mean observation). Overall, we find that the model underestimates the BrO DOAS observations by 40 % on average. This was already indicated in section 3.1.2. when Table 5 was discussed. We have now modified the Abstract, the main text (Sections 3.1.2, 3.2, 3.3.3) and Conclusions to more precisely characterize the discrepancy between observed and modeled BrO columns. In addition, we have made clear that this bias does not significantly impact our regional impact analysis as it has already decreased to 14 % at 40 km.

The authors perform various sensitivity tests to analyse the impact of a number of parameters on the reactive bromine cycle (vertical depth of the plume, formation of NO_x by high temperature chemistry, sulfate aerosol density). These sensitivity tests show that none of these parameters can explain the large discrepancy reached between model and observations.

The authors conclude that the ozone depletion modeling scheme implemented in their model is the likely source of this discrepancy. They notice that all of the ozone gets consumed in their model, thereby limiting the formation of BrO in the near-downwind plume in the model. Unfortunately, the present analysis does not bring clues toward a solution to this problem. Instead of performing an analysis that largely reproduces previous findings, the authors should attempt to discuss the potential role played by the various factors involved in the ozone depletion modeling scheme (ingredients, reactions, feedbacks, etc), so as to point more specifically the likely processes responsible for this modeling bias.

1) As noted by the reviewer, our study is the first 3D regional model study of volcano degassing taking into account volcanic plume chemistry and in particular reactive halogen chemistry. Therefore, we think that it is necessary to investigate whether our newly developed 3D model is able to reproduce some salient features of plume chemistry revealed previously by observations and explained by 1D model studies (i.e. previous findings) such as: BrO/SO₂ trends with distance from the crater and across the plume and the need for the high temperature initialization to reproduce the kinetic of BrO formation.

2) However, we also believe that our work is a progress compared to previous 1D plume studies :

(i) we make a "point-by-point" comparison of the modeled BrO to DOAS observations in transects made across the plume at different distances downwind i.e. each measured data point is compared with its temporally and spatially interpolated model counterpart (Figure

3, 4 and Table 5). This allows a fully quantitative comparison. Previous 1D model studies have only made a quantitative comparison to reported bulk downwind BrO/SO₂ usually as an average of observations with relatively large error bar (e.g. Bobrowski et al., 2007, von Glasow et al., 2010; Roberts et al., 2014; Bobrowski et al., 2015) and made only a qualitative comparison to the reported increase in BrO/SO₂ at the plume edge. Our approach combining 3D high resolution simulations and “point-by point” comparison to the DOAS data is now emphasized in the Abstract, the Introduction and the Conclusion. Note that to avoid some repetitions, we had to make some slight additional modifications to the abstract.

(ii) In addition, we have the potential to make the link between local scale observations close to the volcanic source and regional scale observations given by satellite data. We show that simulated SO₂ columns, when initialized with the Ambrym SO₂ source strength estimate derived from the DOAS observations by Bani et al. (2009) and (2012), agree within 25 % with the SO₂ columns detected by OMI. This is now highlighted in the section 4.1.

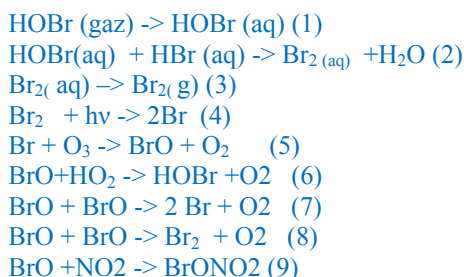
3) Concerning more specifically, the discrepancy on BrO, that is now better characterized in the manuscript as explained above:

(i) We do not agree with the sentence : “*The authors conclude that the ozone depletion modeling scheme implemented in their model is the likely source of this discrepancy*”

Indeed, the chemistry reaction scheme for BrO formation and ozone depletion in volcanic plumes is relatively well established (e.g., Roberts et al., 2009; von Glasow et al., 2009; Von Glasow, 2010; Roberts et al., 2014a.). Most of the gas and photolytic reactions are well known. Note that there are some uncertainties in Brx-NO_x coupling. We choose not to include BrNO₂ following the findings of Roberts et al. (2014a) who includes a detailed BrNO₂ chemistry. Indeed, they find that BrNO₂ does not build up in the plume in contrast to von Glasow (2010) who had a more simplified BrNO₂ chemistry. There are also some uncertainties in the gas-aerosol reactions as highlighted by Roberts et al. (2014b) but our sensitivity study varying aerosol loading (that can alternatively be seen as equivalent to keeping aerosol constant and varying the gas-aerosol reaction) showed no improvement to the model-observation comparison. This was added in section 3.3.3 (see further below).

Instead, we conclude that the lack of ozone is possibly the reason for discrepancy as ozone is a requirement for BrO formation and is also destroyed during the BrO formation.

The following key set of reactions takes place in volcanic plume chemistry, as we now explain in the manuscript:



Because BrO can be photolyzed and the resulting O quickly react with O₂ to give O₃, the key ozone destruction steps are reaction 5 together with reactions 6, 7, 8, 9 (von Glasow et al., 2009). In strong (i.e. near-source and under high emissions) volcanic plumes, gas-phase cycling between Br and BrO (reactions, 5, 7 and 8) is a particularly important cause of ozone depletion. The subsequent lowering of ozone concentration limits the partitioning of BrO from Br. Hence BrO concentrations must become limited by lack of ozone. This is particularly important in the core of the plume, where there is less mixing with background air.

We have now added a section (section 2.1.2) where volcanic plume chemistry is briefly presented to help the reader follow our analysis of simulated plume chemistry and understand the limiting factors on BrO formation. We have also added a paragraph at the end of section 3.2 where we explain in detail the limitation on BrO due to the lack of ozone and refer to the reactions presented in the new section 2.1.2.

(ii) It is important to note that Bobrowski et al. (2015) also found in their model 1D runs of Nyiragongo's plume that BrO formation is ozone-limited in the concentrated plume. They also conclude that BrO and SO₂ do not provide enough information to test model simulations and they claim that measurement of ozone should be a priority for next measurements campaigns. We have added these comments at the end of section 3.3 (sensitivity studies).

(iii) We have now better explained our rationale in section 3.3 dedicated to sensitivity studies.

Our analysis based on model results, in particular Br speciation along the plume in the core and at the edges, indicates that BrO formation is limited due to ozone depletion. But, we have made some assumptions in the modeling of certain processes due to the lack of information to constrain the model or technical limitations. Therefore, we test whether the uncertainties in the representation of these processes could affect the model results and explain the discrepancies found between simulations and observations for the closest transects (~15-20 km) from the vents. More specifically, we focus on the depth of the plume that controls the degree of vertical mixing between emissions and background air, the formation of NO_x by the high temperature chemistry and the surface aerosol area that can affect the in-plume chemistry.

In addition, we have rewritten most of section 3.3.1 (sensitivity to vertical depth) and 3.3.3 (sensitivity to aerosol loading) to clarify these studies. In particular, in section 3.3.1, we explain that increasing the vertical depth of the plume is equivalent to increase the degree of mixing between background air and volcanic emissions.

In section 3.3.3, we have also now mentioned that this sensitivity study is equivalent to increase the HOBr reactive uptake coefficient on sulfate aerosols, while keeping constant the aerosol surface area, for which large uncertainties exist. As mentioned by Reviewer 1, large uncertainties exist on heterogeneous chemistry. Note that the description of the simulated aerosol surface density has now been moved to Section 2.3.2.

(iv) We have also added a paragraph at the end of section 3.3 on an additional sensitivity study that we did not perform but that was done in two other studies and that can be interesting to our study. It is the role of total bromine emissions.

Here is this new paragraph

“Note that we did not test the sensitivity of the model results to the strength of total bromine emissions. Increasing total bromine emissions would increase total bromine in the plume. But because of the ozone limitation, this would lead to a reduced fraction of BrO and an increased fraction of Br. Finally, these two effects would compensate as found with a 1D model for the Nyiragongo’s plume by Bobrowski et al. (2015). As a result, increasing total bromine emissions would not impact BrO columns. This compensation was also found by Roberts et al. (2014) with their 1D model when compared their “high” and “medium” total bromine scenarios.”

(v) Concerning the comment of the reviewer : we could not find a solution to the discrepancy. We consider that it is a challenging problem to simulate volcanic BrO. Compared to previous studies, our model-observation comparison is particularly quantitative and in a way can highlight more the discrepancies. In addition, with a 3 D model, transport, mixing and concentrations in background air are not tuned by the user as they are in 1D models. We consider that we went as far as we could with these sensitivity studies. It is important to note that our study suffers from a lack measurements other than BrO and SO₂, even though our choice of Ambrym 2005 as a case study makes use of rather unique aircraft dataset of DOAS transects up to 40 km downwind. The main point is that BrO and SO₂ are not sufficient to fully constrain our modeling of volcanic plume chemistry as also highlighted in Bobrowski et al. (2015). This was already highlighted in the Conclusions but we have added it at the end of section 3.3.

(vi) We also consider it is important to mention that inaccuracies in DOAS retrievals can also affect the comparison. Under volcanic plume conditions (especially strong plumes as found during this extreme degassing event and close to the vents), it is well known that DOAS retrievals can suffer from inaccuracies. These have been estimated to some extent (e.g. Kern et al. 2010; Kern et al., 2012, Bobowski et al., 2010), focusing on SO₂. There remains a need to better understand DOAS uncertainties especially also for BrO.

In a second part (section 4), the impact of Ambrym sulfur- and halogen-rich emissions on sulfate aerosol, bromine and ozone content (section 4.2) at regional scale is proposed, as well as their impact on the lifetimes of methane and sulfate aerosols (section 4.3). However, it is difficult for the reader to evaluate the relevance of these regional analyses for multiple reasons :

- First, the uncertainty on the BrO content found in the first section, which is substantial given the three-fold discrepancy between modelled and observed BrO, is not put forward neither discussed to evaluate uncertainties on results at a regional scale.

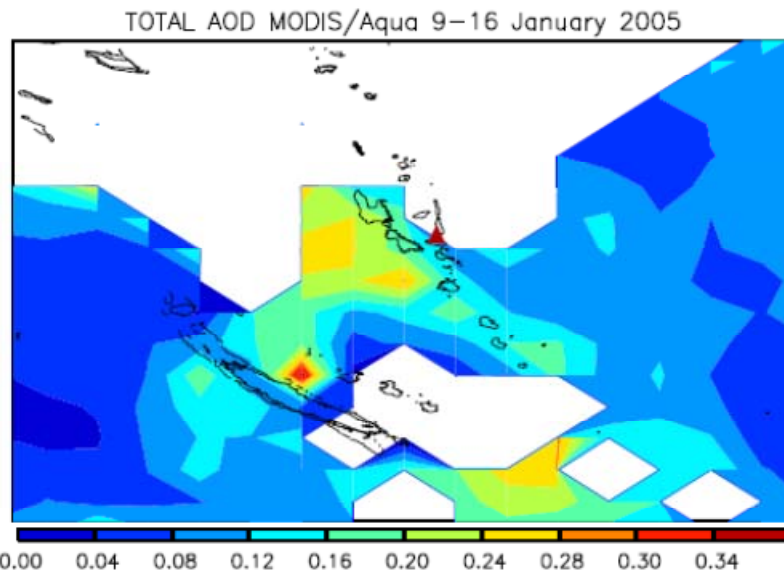
As mentioned earlier, we find a three-fold discrepancy when we compare the maximal BrO columns measured around 15 km of the vents with the corresponding modeled counterparts. Overall, the mean difference between BrO columns reported by Bani et al. (2009) and those simulated in our main simulation S1_HighT is about 40%, as indicated in section 3.1.2 and Table 5. For the furthest transect (40 km of the vents), the mean difference between observed and modeled columns is only of 14%. As a result, we believe that this small bias would not

significantly impair the regional impact study. This is now explicitly stated at the end of Section 3 before studying the impact of the Ambrym volcano at the regional scale.

- Second, this section does not present any observation which could allow for testing the robustness (not to say the reliability) of these results. Satellite observations of aerosols (such as MODIS, POLDER, etc...) could be explored to better constrain model results.

- (i) We agree with the reviewer that the scarcity of data is a major challenge in the study of volcanic halogen Ambrym impacts. Nevertheless, in the section 4.1, we had presented a comparison between OMI SO₂ columns on 12th of January 2005 at 02:30 UT and the spatially and temporally interpolated model counterparts (Figure 10). We have now modified the text in the section 4.1 to present a more quantitative comparison. In particular, we have now calculated statistical quantities as the figure of merit in space (FMS) that quantifies the degree of spatial matching between observed and simulated plumes and the bias between the magnitudes of observed and modelled mean SO₂ columns. This comparison shows that we are able to reproduce fairly well the direction and the width of the plume at the regional scale as well as in good extent the magnitude of the SO₂ columns and give better confidence to our modeling.
- (ii) We agree that satellite data are available regarding sulfate aerosol. In the section 4.2, we have now added a plot showing the Total Aerosol Optical Depth from MODIS/aqua at 0.55 microns (see below). We have used the eight day average gridded L3 product from MODIS/Aqua (MYD08_E3) for 9-16 January 2005. We have added a paragraph in section 4.2 : “Total aerosol optical depth (AOD) at 550 nm is also shown in Figure 5S of supplementary material for the 9-16 January 2005. Enhanced AOD are clearly seen southeast of Ambrym in the direction taken by the plume the 12th January 2005 as discussed earlier (see Figure10) as well as northwest of Ambrym in the direction of trades winds. The latter point is again consistent with OMI SO₂ images from GSFC (Goddard Space Flight Center) at http://so2.gsfc.nasa.gov/pix/daily/0105/vanuatu_0105z.html showing that the plume was carried toward the northwest on the 14th and 15th January 2005. Enhanced AOD values varies between 0.12 and 0.34, which are approximately twice higher than the 3 years average (Oct.2005-Oct.2008) AOD presented by Lefevre et al. (2015). This is consistent with the extreme passive degassing activity of Ambrym during January 2005. This confirms the strong influence of Ambrym on the budget of

sulfate aerosol in the South West Pacific region and is qualitatively in agreement with our



results. “

- Thirdly, according to the abstract and section names, the reader would expect that this second section would consist in an evaluation of the longer-term regional impact of Ambrym emissions that would generalize the study performed in the first part of the paper for a single day of emission (12 Jan 2005). However, Section 4 is only restricted to the same single event/day. Instead, the authors may broaden the scope of the study by assessing the impact of the continuous emissions of Ambrym.

(i) We agree that a full assessment of regional scale impacts cannot be achieved by analysis of one day of simulation (there were 11 days of spin-up). But, we had strong computational limitations. Indeed, our simulations that include detailed chemistry and several nested grids are very demanding in term of computing time. We also believe that our study that includes model development, model evaluation at the plume level, sensitivity tests, a first investigation of plume chemistry on the regional scale and its implications for the troposphere was a substantial undertaking. For these reasons to make longer-term model runs of many months/years for a full assessment of impacts (to be repeatedly undertaken for a sensitivity study) would be a substantial second piece of work.

(ii) Moreover, our paper confirms that the impact of Ambrym is regional and not only local in term of sulfur compounds. But it also stresses the role of halogen reactive chemistry at the regional scale. Indeed, we calculate significant bromine enhancement and ozone depletion at the regional scale up to thousand of kilometers of Ambrym. We have also shown evidence for bromine transport into the upper troposphere by convection. The influence of reactive halogen chemistry on the oxidizing power of the atmosphere is also demonstrated as well as on the lifetime of volcanic SO_2 and hence on sulfate production. This leads us to conclude that these halogen volcanic emissions and their associated chemistry need to be considered when studying the influence of volcanic emissions on climate. This is a point which is important and not yet well recognized in the atmospheric-volcanic community. Our study provides the evidence to motivate and guide future halogen-chemistry-climate assessments.

- Finally, the Vanuatu region is often cloudy. The formation of sulfate aerosol in aqueous-phase may not be negligible in this context. However, this process is not included in the model. The authors should mention this potential issue, which may significantly impact the modeling results.

We agree that the formation of sulfate in aqueous phase might be important, and that this is a limitation of our study. This issue was already mentioned in the manuscript: Section 2.3.1 “The sulfur scheme includes gas-phase oxidation, and dry and wet deposition, but not aqueous-phase oxidation.”

Section 4.2.1 “In this model study, the aqueous-phase oxidation of SO₂ to sulfate was not taken into account. This process becomes self-limiting in strong volcanic plumes due to the titration of oxidants for example H₂O₂ (Schmidt et al., 2010) but may have a significant contribution to sulfate formation over the whole model domain thus will be considered in future work.”

Section 4.4 “Our regional 3D model study includes a less detailed SO₂-sulfate chemistry scheme (gas-phase oxidation only) but includes detailed plume reactive halogen chemistry.”

This is further emphasized in the revised version of Section 4 and Conclusions as a model limitation and an area of future improvement. Specifically we have now added, as the reviewer mentioned, that this process may be of particular importance because the Vanuatu region is particularly cloudy (provided the aqueous-oxidation is not self-limiting i.e. in relatively dilute plumes)

While significant effort has been undertaken by the authors to include reactive halogen chemistry in a 3D chemistry-transport model, the manuscript is lengthy and relatively difficult to follow for the reader. According to me, this article would benefit to be divided in two papers (possibly a companion paper).

- The first paper would require more developments on the modeling aspects in order to find a better first-order agreement between modeled and observed downwind BrO abundances, which represents the critical observations of this study. At least should the model processes responsible for model biases be listed and discussed in details.

We have already replied above to all these aspects. We summarize here our answer.

First, overall the mean difference between BrO columns reported by Bani et al. (2009) and those simulated in S1_HighT is about 40% (relative to the observations) as indicated in section 3.1.2. We consider that this is a reasonable result under the conditions of our study. The bias is more pronounced (60%) for the transect closest to the source but small further downwind around 14%.

Secondly, with the model, we have done a thorough analysis of the plume chemistry by looking at Br speciation evolution in the plume at the edge and in the core that leads us to identify that the lack of ozone in the simulation in the plume limits the partitioning of BrO from Br as explained above.

Thirdly, we have tested whether a misrepresentation of some model processes (due to a lack of information) could be the reason for the discrepancy. We had identified several processes whose modeling is uncertain and could impact BrO. It was injection height, model mixing, NO_x emissions due to high temperature chemistry and aerosol loading. For this latter process, the sensitivity study was equivalent to perform a sensitivity study on the value of the uptake coefficient. We have also added a discussion on the impact of total bromine emissions.

451 So, we have ruled out the implications of these different processes to explain the discrepancy.
452 We consider that we went as far as we could. We also conclude that measurements of BrO
453 and SO₂ are not sufficient to fully constrain our modeling of volcanic plume chemistry.

454
455 The improvements made in the paper in response to the reviewer were described above when
456 we answered in detail to each question.

457 - *The second paper would require more constraining observations to validate results of*
458 *the impact of halogen-rich emissions at a regional scale. As Ambrym is continuously*
459 *degassing, a longer-term study would be possible, i.e. not restricted to a single day of*
460 *substantial emissions. This would provide a global and more representative estimation*
461 *of the actual regional impact of Ambrym emissions.*

462 We have also replied to this comment above. We summarize our answer here. We agree with
463 the reviewer that a long-term study would be necessary to fully understand the actual regional
464 impact of Ambrym. But it would be a substantial second piece of work, given that our
465 simulations are very demanding in term of computing time. We also think that our study
466 (model development, model evaluation at the plume level, sensitivity tests, a first
467 investigation of plume chemistry on the regional scale and its implications for the
468 troposphere) is already a substantial undertaking. Our study also highlights interesting results
469 on the regional influence of Ambrym. In particular, it emphasizes that reactive halogen
470 chemistry should be considered when studying the impact of volcanic emissions on climate.
471 We have given more details above in our previous answer.

472
473 *Minor comments :*

474 - *Page 35324: sentence in line 1 has to be rephrased.*

475 The sentence was replaced by “Biogenic emissions were provided by a monthly mean
476 climatology for the year 2000 produced with the MEGAN (Model of Emissions of Gases and
477 Aerosols from Nature) database (Guenther et al., 2006).”

478 - *Page 35326, line 23 : ‘Due to*

479 ...

480 *‘ : sentence not ended*

481 It was corrected. The sentence is now : “Due to uncertainty in volcanic NO_x emissions (see
482 discussions of Martin et al., 2012; Roberts et al., 2014a; Surl et al., 2015), HSC Chemistry
483 output both with and without NO_x were used to initialise CCATT-BRAMS (Simulations
484 S1_HighT and S1_HighT_noNO_x).”

485

486 - *Page 35332, line 5 : ‘similar to’ (not ‘than’)*

487 We believe that that the sentence was on page 35331 line5. We have made the correction.

488

489 - *Page 35334, line 26 : remove first ‘reactive’*

490 This was removed.

491 - *Page 35336, lines 26-28 : which are the radicals other than NO_x that you think are*
492 *important ?*

493 We have tested the impact of NO_x emissions on the plume chemistry by comparing two
494 simulations. The first one S1_HighT includes emissions of OH, NO, Cl, Br to take into
495 account high temperature chemistry at the vent in addition to emissions of SO₂, sulfate
496 aerosols and halides HCl and HBr. The second S1_HighT_noNO_x has the same emissions
497 than S1_HighT except that it does not include NO emissions. So by “other radicals” we meant
498 OH, Cl and Br radicals.

This is now clarified earlier in the paragraph. The sentence (previously p35336 18-20) “We performed a simulation (S1_HighT_noNO_x) where from the high-temperature initialization was not included while keeping constant the emissions of the other radicals from HSC” was replaced by this sentence “We performed a simulation (S1_HighT_noNO_x) where NO_x from the high-temperature initialization was not included while keeping constant the emissions of the other radicals (i.e. OH, Cl, Br) from HSC Chemistry.”

The sentence (previously p35336, line 26-28) mentioned by the reviewer became :

“This suggests that NO_x emissions are not crucial to kick off the chemistry initially but that they are responsible for the decline of HBr further downwind after 15 km.”

- Page 35340 : *Could you explain more why the result on sulfate aerosol burden confirms that sulfate which formed from atmospheric oxidation are the main driver of volcanic halogen chemistry ?*

We find that the sulfate burden has increased by 0.08 Tg due to Ambrym emissions since the beginning of the simulation on January 12th. This was calculated by comparing the sulfate burden between S1_HigT and S0. But the total direct emission of sulfate due to Ambrym since the beginning of the simulation reaches 3.34 Gg on January 12th. This cumulated direct emission represents 4% (= 3.34Gg/0.080Tg) of the total burden. It is a maximal value, as these emissions could have been washed out in the model or left the domain of the study.

To clarify, we have modified the sentence “This means that at least 96 % of the sulfate burden increase due to Ambrym results from the atmospheric oxidation of SO₂ from the volcano by OH.” by “This means that at least 96 % ($\approx (80-3.34)/80 \times 100$) of the sulfate burden increase due to Ambrym results from the atmospheric oxidation of SO₂ from the volcano by OH.

- Page 35340, line 14 : replace ‘sulfate is’ by ‘sulfate aerosols are’

This was corrected.

- Page 35340, line 22 : words are attached here ‘HighTand’ but also in several places throughout the text.

This was corrected.

- Table 4 : *what are the sources used to determine the ratios used to initialise the model?*

Ratios from Table 4 are explained in detail in Section 2.3.3:

- HBr/SO₂ and HCl/SO₂ ratios are derived from measurements of Allard et al. (2009).
- H₂SO₄/SO₂ ratios are derived assuming that 1% of sulfur is emitted as H₂SO₄ based on Mather et al. (2003) and on Von Glasow et al. (2009).
- OH/SO₂, NO/SO₂, Cl/SO₂, Br/SO₂ are output from an HSC chemistry simulation initialised with data from Table 3 as explained in Section 2.3.3 where references are given.

We think that we cannot put all these information in the caption of the Table 4. But, we have added “See section 2.3.3 for the detailed explication of the ratios derivation” in the caption of the Table 4. For clarity, we have also rephrased some of the sentences of the Table 4.

We have also added in Table3 that mixing ratios are mass mixing ratios.

Additional corrections from the authors in Abstract, section 4.3 and Conclusion :

We have rephrased the results of section 4.3. Because of the non linearity of the chemistry, we cannot say: “Reactive halogen chemistry is responsible for about 62% of the methane lifetime increase with respect to OH, with depletion of OH by SO₂ oxidation responsible for

the remainder (38%).” Indeed, it is not strictly possible to determine the contribution of one process (for example reactive halogen chemistry) by turning it off and compare with a simulation where the process is taken into account. Indeed, the contribution that we find by doing this, for instance 62% here, is not necessarily right because of the non linearity of the chemical system. So we replace the sentence in the abstract the sentence by “When considering reactive halogen chemistry, the lengthening of methane lifetime with respect to OH is increased by a factor of 2.6 in our simulation compared to a simulation including only SO₂ emissions” . Similar sentences are now in the main text (section 4.3), Abstract and Conclusion.

For the same reason, we have rephrased “The reactive halogen chemistry in the plume is also responsible for an increase of 36% of the SO₂ lifetime with respect to oxidation by OH” by “Including the reactive halogen chemistry in our simulation increases the lifetime of SO₂ in the plume with respect to oxidation by OH by 36% compared to a simulation including only volcanic SO₂ emissions”.

Changes in the manuscript highlighted by the track changing :

~~Modeling the evolution and the local and regional impacts of the~~ reactive halogen plume
from Ambrym ~~volcano~~ and its impact on the troposphere with the CCATT-BRAMS
mesoscale model ~~CCATT-BRAMS~~

L. Jourdain¹, T.J. Roberts¹, M. Pirre¹, B. Josse²

[1]{ Laboratoire de Physique et de Chimie de l’Environnement et de l’Espace (LPC2E),
Université d’Orléans, CNRS, Orléans, France}

[2]{ CNRM-GAME, Météo-France and CNRS, Toulouse, France}

Correspondence to: L. Jourdain (line.jourdain@cnrs-orleans.fr)

Abstract:

Ambrym volcano (Vanuatu, Southwest Pacific) is one of the largest sources of continuous
volcanic emissions worldwide. As well as releasing SO₂ that is oxidized to sulfate, volcanic
plumes in the troposphere are shown to undergo reactive halogen chemistry whose

Mis en forme : Espace Après : 10 pt

atmospheric impacts have been little explored to date. Here, ~~two-way nested simulations were~~
~~performed~~ we investigate with the regional scale model CCATT-BRAMS ~~to test our~~
~~understanding of the volcano plume~~ chemical processing ~~and to assess~~ in the Ambrym plume
~~and the~~ impact of ~~Ambrym~~ this volcano on the atmospheric chemistry at both local and
 regional scales. We focus on an episode of extreme passive degassing that occurred in early
 2005 and for which airborne DOAS measurements of SO₂ and BrO columns, in the near
 downwind plume between 15 and 40 km from the vents, have been reported. The model was
 developed to include reactive halogen chemistry and a volcanic emission source specific to
 this extreme degassing event. ~~SO₂ simulated~~ In order to test our understanding of the volcanic
plume chemistry, we performed very high resolution (500 m x 500 m) simulations using the
model nesting grid capability and compared “point-by-point” each DOAS measurement to its
temporally and spatially interpolated model counterpart. Simulated SO₂ columns show very
 good quantitative agreement with the DOAS observations ~~as well as with OMI data,~~
 suggesting that the plume direction as well as its dilution in the near downwind plume are
 well ~~represented. Simulations are presented with and without~~ captured. The model also
reproduces the salient features of volcanic chemistry as reported in previous work such as
HO_x and ozone depletion in the core of the plume. When a high-temperature chemistry
initialization ~~that includes radicals formed by high-temperature partial oxidation of magmatic~~
~~gases by ambient air. When is~~ included high-temperature chemistry initialization, the model is
 able to capture the observed BrO/SO₂ trend with distance from the vent ~~in the near downwind~~
~~plume. However, the maximum of.~~ The main discrepancy between observations and model is
the bias between the magnitudes of observed and simulated BrO columns ~~enhancement is still~~
~~underestimated by a factor 3. The model identifies~~ that ranges from 60 % (relative to the
observations) for the transect at 15 km to 14 % for the one at 40 km from the vents. We
identify total in-plume depletion of ozone ~~(15 ppbv)~~ as a limiting factor to the partitioning of

Mis en forme : Anglais (Royaume-Uni)

Mis en forme : Anglais (Royaume-Uni)

Mis en forme : Anglais (Royaume-Uni)

605 reactive bromine into BrO₂, ~~of particular importance in this very strong plume at~~ in the near
 606 source (concentrated) plume under these conditions of extreme emissions and low
 607 background ozone ~~conditions—concentrations (15 ppbv).~~ Impacts of Ambrym in the
 608 Southwest Pacific region were also ~~evaluated~~ analyzed. As the plume disperses regionally,
 609 reactive halogen chemistry continues on sulfate aerosols produced by SO₂ oxidation and
 610 promotes BrCl formation. Ozone depletion is weaker than at the local scale but still between
 611 10 % to -40% , in an extensive region a few thousands of kilometres from Ambrym. The
 612 model also predicts transport of bromine to the upper troposphere and stratosphere associated
 613 with convection events. In the upper troposphere, HBr is re-formed from Br and HO₂.
 614 Comparison of SO₂ regional scale model fields with OMI satellite SO₂ fields confirms that the
 615 Ambrym SO₂ emissions estimate based on the DOAS observations used here is realistic.

Mis en forme : Anglais (États Unis)

Mis en forme : Non Exposant/ Indice

Mis en forme : Anglais (Royaume-Uni)

616 The model confirms the potential for volcanic emissions to influence the oxidizing power of
 617 the atmosphere: methane lifetime (calculated with respect to OH and Cl) is overall increased
 618 in the model due to the volcanic emissions. ~~Reactive~~ When considering reactive halogen
 619 chemistry ~~is responsible for about 62%, that depletes HOx and ozone, the lengthening of the~~
 620 methane lifetime increase with respect to OH ~~with depletion is increased by a factor of OH~~
 621 by 2.6 compared to a simulation including only volcanic SO₂ oxidation responsible for the
 622 remainder (38%)—emissions. Cl radicals produced in the plume counteract 41% of the
 623 methane lifetime lengthening due to OH depletion. ~~The~~ Including the reactive halogen
 624 chemistry in ~~the plume is~~ our simulation also ~~responsible for an increase of 36% of~~ increases
 625 the SO₂-lifetime of SO₂ in the plume with respect to oxidation by OH by 36% compared to a
 626 simulation including only volcanic SO₂ emissions. This study confirms the strong influence of

Mis en forme : Anglais (Royaume-Uni)

Mis en forme : Anglais (Royaume-Uni)

Mis en forme : Anglais (Royaume-Uni)

Mis en forme : Anglais (Royaume-Uni)

Mis en forme : Anglais (Royaume-Uni)

Mis en forme : Anglais (Royaume-Uni)

Mis en forme : Anglais (États Unis)

627 Ambrym emissions during the extreme degassing event of early 2005 on the composition of
 628 the atmosphere at ~~the~~ both local and regional scales. It also stresses the importance of

629 considering reactive halogen chemistry when assessing the impact of volcanic emissions on
630 climate.

Mis en forme : Anglais (Royaume-Uni)

631

632

633

634 1. Introduction

635 Volcanic activity is a source of climatically and environmentally important gases and aerosols
636 in the atmosphere. To this respect, much work has ~~been focusing~~focused on the climate
637 impact of sulfur compounds injected by major volcanic explosions ~~that inject directly and~~
638 ~~massively sulfur compounds~~ into the stratosphere. In this layer, ~~the~~they are converted into
639 sulfate aerosols that have a long residence time (~1-2 years) and can affect climate directly
640 via the perturbation of the Earth's radiation balance -as well as indirectly due to the strong
641 coupling between radiation, microphysics and atmospheric chemistry in the stratosphere. This
642 forcing from volcanic stratospheric aerosols is now well understood and is thought to be the
643 most important natural cause of externally forced climate change on the annual but also on the
644 multi-decadal time scales and hence ~~can~~is thought to explain the majority of the pre-industrial
645 climate change of the last millennium (Myrhe et al., 2013).

646 On the other hand, the impact of other compounds as halides (HCl, HBr) injected by
647 explosive eruptions into the stratosphere as well as the overall impact of minor eruptions and
648 quiescent passive degassing have been largely overlooked. However, the presence of volcanic
649 halogens in the stratosphere following explosive eruptions has been recently detected (e.g.,
650 Hunton et al., 2005; Rose et al., 2006; Prata et al., 2007; Theys et al., 2014, Carn et al.,
651 2016). Such volcanic halogen injection, enabled by incomplete volcanic halides washout as
652 first predicted by a model study (Textor et al., 2003), was found to cause enhanced reactive

chlorine and bromine as well as enhanced ozone depletion (Rose et al., 2006; Millard et al., 2006). As a result, it is important, as emphasized in Cadoux et al. (2015), to consider volcanic halogens in addition to sulfur compounds when studying the influence on the stratosphere of past and future explosive eruptions.

Until recently, the impact of quiescent degassing and of minor eruptions have also been largely overlooked because of the lower lifetime of volcanic emissions in the troposphere, ~~the climate impact of quiescent degassing and minor eruptions has been less studied. However,~~ However, it was shown that quiescent degassing alone is responsible for a high proportion (~30–70 %) of the volcanic SO₂ flux to the atmosphere (Andres and Kasgnoc, 1998; Halmer et al., 2002; Mather et al., 2003). In addition, quiescent degassing as well as minor eruptions were found to contribute more to the sulfur load in the free troposphere in regard to their emissions compared to stronger ~~sources as~~ oceanic and anthropogenic sources due to the elevation of most volcanoes (e.g., Chin and Jacob, 1996; Graf et al., 1997). Furthermore, recent studies show the need for a better knowledge of the tropospheric concentrations of natural aerosols and their precursor gases to quantify the aerosol indirect forcing from anthropogenic activities due to nonlinearities in the relations linking aerosol concentrations and cloud albedo (Carslaw et al., 2013; Schmidt et al., 2012). Volcanic emissions in the troposphere have also been recognized to cause environmental and health problems due to the deposition of SO₂, sulfate, hydrogen halides (mainly HCl and HF) and toxic metals (for a review, see Delmelle, 2003) as well as adversely impacting air quality. ~~Moreover~~

Finally, there is also evidence of chemical reactivity in tropospheric plumes with consequences on the oxidizing power of the troposphere (and hence effects on ~~the~~ climate) as well as on the deposition of mercury (e.g., von Glasow, 2010). Indeed, reactive ~~halogen~~ halogens as BrO (e.g., Bobrowki et al., 2003; Lee et al., 2005; Oppenheimer et al., 2006; Bobrowski and Platt, 2007; Bani et al., 2009; Kern et al., 2009; Theys et al., 2009;

678 Boichu et al., 2011; Kelly et al., 2013; Hörmann et al., 2013; Bobrowski et al., 2015) as well
 679 as OCIO (Bobrowski et al., 2007; General et al., 2014, Gliß et al., 2015) have been detected in
 680 the ~~plume~~[plumes](#) of many volcanoes worldwide. Observations of ClO have also been
 681 reported (Lee et al., 2005) but are subject to some uncertainties (see Roberts et al., 2009). For
 682 BrO, it is clear that its formation results from the conversion of the emitted volcanic HBr gas
 683 into reactive bromine in the presence of sulfate aerosols (Oppenheimer et al., 2006,
 684 Bobrowski et al., 2007, Roberts et al., 2009, Von Glasow, 2010). ~~The plume atmospheric~~
 685 ~~chemistry is also highly influenced by the degree of plume mixing with entrained ambient air~~
 686 ~~(Roberts et al., 2014a)~~. Central to this chemical mechanism, first identified in the context of
 687 arctic spring ozone depletion ~~event~~[events](#) (Fan and Jacob, 1992), is the reactive uptake of
 688 HOBr ~~in~~[on](#) the sulfate aerosol. The net result is ~~bromide~~ release ~~from the sulfate aerosol to~~
 689 ~~form~~[of](#) gaseous reactive bromine [from the sulfate aerosol](#) (initially as Br₂, which then
 690 converts into other forms including Br, BrO, HOBr, BrONO₂) and depletion of oxidants O₃,
 691 HO₂ as well as NO₂. Reactive bromine acts as a catalyst to its own formation, leading to an
 692 exponential growth called “bromine explosion” also observed in the arctic during spring (e.g.,
 693 Barrie et al., 1988), in the marine boundary layer (e.g., Saiz Lopez et al., 2004) and over salt
 694 lakes (e.g., Hebestreit et al., 1999) (for [a](#) review see Simpson et al., 2015). Following the
 695 first discovery of volcanic BrO (Bobrowski et al., 2003), depletion of ozone has also been
 696 observed in volcanic plumes (Vance et al. 2010; Oppenheimer et al. 2010; Schuman et al.,
 697 2011; Kelly et al., 2013; Surl et al. 2015). ~~The plume atmospheric chemistry is also highly~~
 698 ~~influenced by the degree of plume mixing with entrained ambient air (Roberts et al., 2014a).~~
 699 Owing to the numerous environmental and climate impacts of quiescent degassing and minor
 700 eruptions occurring in the troposphere, it is important to take these volcanic sources into
 701 account in the 3D atmospheric models (regional and global models) that aim to understand the
 702 chemical composition of the atmosphere, its evolution and its interaction with climate. This

703 paper is an attempt to do that and builds on previous modeling work. -The numerical 1D
704 models MISTRA and PlumeChem (e.g., Bobrowski et al., 2007; Roberts et al., 2009, 2014a;
705 von Glasow et al., 2010; -Boichu et al. 2011; Kelly et al., 2013) are able to broadly reproduce
706 ~~observations of the~~observed ratios of BrO to SO₂ with distance downwind from ~~the craters~~
707 volcanoes as well as simulate ozone depletion (e.g., Roberts et al., 2014a; Surl et al., 2015).
708 These modeling studies show the need to take into account the high temperature chemistry
709 following the mixing of volcanic gas with ambient air in order to reproduce the timing of BrO
710 formation. Indeed, high-temperature model studies (Gerlach, 2004; Martin et al., 2006;
711 Martin et al., 2009) have predicted that the mixing of volcanic gases and air at the vent leads
712 to high temperature oxidative dissociation and hence to the formation of radical species.
713 These species accelerate the onset of this chemistry, the formation of BrO being
714 autocatalytical and driven forwards by low-temperature reactions occurring on volcanic
715 aerosol. To date, simulations of reactive halogen (BrO_x, ClO_x) chemistry in volcanic plumes
716 and its impacts have been restricted to 1D and box model studies.

717 Here, we present a 3D regional model study of the impact of Ambrym volcano emissions, not
718 only of sulfur emissions but also of halogen emissions including their reactive chemistry, on
719 the chemical composition of the troposphere at both local and regional scales. Ambrym
720 volcano, Vanuatu, - is recognized as a significant contributor to the global volcanic flux of SO₂
721 (Bani et al., 2012; Allard et al., 2009, 2015) as well as of halogen halides HF, HCl, HBr
722 (Allard et al. 2009, 2015). Our focus is an extreme degassing episode that occurred in early
723 2005, for which airborne DOAS SO₂ and BrO columns in the plume (15- 40 km of the vents)
724 have been reported (Bani et al., 2009).

725 The paper is organised as follows. In section 2, we briefly present the Ambrym volcano, ~~and~~
726 the main chemical reactions of volcanic plumes. We also present the reported measurements
727 and detail the model developments made in this study. In section 3, we first test our

understanding of the plume chemistry at the plume level by comparing “point by point” the model simulations with the DOAS SO₂ and BrO columns in the near downwind plume and as well as performing some sensitivity studies. The local impact of Ambrym plume is also presented. In section 4, the regional impact of Ambrym plume is calculated and analyzed and discussed. The conclusions are presented in section 5.

2. Methods

2.1 The Context: Ambrym volcano and volcanic plume chemistry

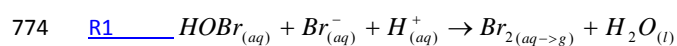
2.1.1 Ambrym volcano

The Vanuatu Arc is a group of about 80 islands and islets located in the Southwest Pacific that was formed and had continued to evolve as a result of the complex interaction between the Pacific plate and the Indo-Australian plate (Robin et al., 1993). Ambrym (160°08'E, 16°15'S) situated in the central zone of the Vanuatu arc is a basaltic stratovolcano of 50 km long and 35 km wide rising 1334 meters above sea level. It has in its center a 12 km diameter caldera with two active cones Mounts Marum and Benbow filled with permanent lava lakes. It has been recently highlighted that the Vanuatu arc is one of the most important entry points for volcanic gases into the atmosphere with mean annual emission of 3Tg/yr of SO₂ estimated for the period 2004-2009 representing about 20 % of the global volcanic SO₂ annual emissions (Bani et al., 2012). Under normal quiescent degassing conditions, Ambrym volcano has a mean emission of 5.44 kt/day of SO₂, comparable with Mt Etna (Italy), and hence contributes to two-thirds of the total budget of the arc (Bani et al., 2012). It is also a significant contributor to the global volcanic flux for several other species (Allard et al., 2009; 2015). The volcano impact on the population and environment includes crop damage and food shortages due to deposition of halogen acids, SO₂ and H₂SO₄ as well as dental fluorosis due to the water contamination by wet deposition of fluorine (Allibone et al.,

2010). The volcano impact on sulfate aerosol in the Southwest Pacific has also recently been investigated (Lefèvre et al., 2015). They found a strong signal in the aerosol optical depth (AOD) from MODIS (Moderate Resolution Imaging Spectroradiometer) due to Ambrym sulfur emissions; this signal contributes ~~for~~ 15 % to the total AOD as far as 1500 km from the volcano. Here, we focus on the halogen impact alongside sulfur. We study an event of extreme passive degassing that took place in January 2005 when the SO₂ emission was ~~more~~ than 3 times higher ~~that~~ than its mean value over the 2004-2009 period (Bani et al. 2012). This extreme degassing occurred as a pulse of several months duration (Bani et al., 2012). Our study evaluates impacts from the continuous degassing on 12th January, enabling comparison to plume BrO and SO₂ measurements from a field campaign (Bani et al., 2009).

2.1.2 Volcanic plume chemistry

Reactions R1-R7 illustrate the autocatalytic conversion of volcanic HBr into reactive bromine species and the associated catalytic ozone depletion (for a more complete set of reactions, see Simpson et al., 2007). A key reaction is the heterogeneous reaction of HOBr with Br⁻ (from dissolved volcanic HBr) and H⁺ in volcanic sulfate aerosols (R1) that results in the production of Br₂. Once released to the gas-phase, Br₂ is rapidly photolysed to give 2 Br radicals (R2), which can react with ozone to form BrO (R3). The reaction of BrO with HO₂ (R5) reform HOBr that can again react on the sulfate aerosol (R1) to further propagate the cycle, each time doubling the concentration of reactive bromine. In addition to reactive uptake of HOBr, hydrolysis of BrONO₂ (R7) into sulfate aerosol can also regenerate HOBr that can undergo another cycle.



Code de champ modifié

Code de champ modifié

776 R3 $Br + O_3 \rightarrow BrO + O_2$

Code de champ modifié

777 R4a $BrO + BrO \rightarrow 2Br + O_2$

Code de champ modifié

778 R4b $BrO + BrO \rightarrow Br_2 + O_2$

Code de champ modifié

779 R5 $BrO + HO_2 \rightarrow HOBr + O_2$

Code de champ modifié

780 R6 $BrO + NO_2 \rightarrow BrONO_2$

Code de champ modifié

781 R7 $BrONO_2 + H_2O(l) \rightarrow HOBr + HNO_3$

Code de champ modifié

782 Because BrO can be photolyzed and the resulting O quickly reacts with O₂ to give back O₃,
783 the key ozone destruction steps are reactions R3 together with reactions R4a, R4b, R5 and R6
784 (von Glasow et al., 2009). Note, that BrCl can be the product of the reactive uptake of HOBr
785 (R8) when Br⁻ becomes depleted, leading to non-autocatalytic formation of reactive chlorine.

786 R8 $HOBr_{(aq)} + H^+_{(aq)} + Cl^-_{(aq)} \rightarrow BrCl_{(aq \rightarrow g)} + H_2O_{(l)}$

Code de champ modifié

787 ▲

Mis en forme : Police :Gras, Couleur
de police : Automatique

788 2.2 Measurements

Mis en forme : Espace Avant : 1,5 pt

789 2.2.1 DOAS Data

790 We use DOAS (Differential Optical Absorption Spectroscopy) measurement of SO₂ and BrO
791 columns performed in the plume of Ambrym during the episode of extreme passive degassing
792 the 12th January 2005 (Bani et al., 2009). The measurements were made between 5 and 6h UT
793 onboard of an aircraft flying just below the Ambrym plume (at 500-1000 m above the sea
794 level) in the cross-wind direction (15-40 km south east of the craters) with the instrument's
795 telescope pointing to zenith. The procedure to retrieve the columns is described in Bani et al.
796 (2009) and Bani et al. (2012). Reported errors (2σ) on the SO₂ and BrO retrieved columns are
797 respectively ±52 mg m⁻² (i.e. 4.89 e⁺⁶10¹⁶ molecules/cm²) and ±0.39 mg m⁻² (i.e. 2.44 e⁺⁴10¹⁴
798 molecules/cm²). In the present study, these data are used to evaluate the simulation of

799 volcanic plume chemistry. Note that these data in conjunction with wind estimates were used
800 by Bani et al. (2009) to estimate Ambrym SO₂ emission rate (18.8 kt/day).

801

802 **2.2.2 OMI Data**

803 The Ozone Monitoring instrument (OMI) is a nadir viewing UV/visible CCD spectrometer
804 sampling a swath of 2600 km with a ground footprint of 13 km x 24 km, launched aboard
805 the ~~NASA's~~[NASA](#) Aura satellite in July 2004 (~~Barthia~~[Bharthia](#) and Wellemeyer, 2002). Here,
806 we use the planetary boundary layer (PBL) level-2 SO₂ column amount product derived with
807 the principal component analysis (PCA) algorithm (Li et al., 2013). Only data with scenes
808 near the center of the swath (rows 5-55) with radiative cloud fraction less than 0.3 and with
809 ozone slant column lower than 1500 DU were considered as recommended. Noise and biases
810 in retrievals are estimated at ~0.5 DU for regions between 30°S-30°N.

Mis en forme : Indice

811

812 **2.2.3 MODIS data**

813 The Moderate Resolution Imaging Spectroradiometer (MODIS) was launched aboard the
814 NASA's Aqua satellite in May 2002. MODIS instrument measures spectral radiances in 36
815 high spectral resolution bands between 410 to 14400 nm, sampling a swath of 2330 km
816 (Remer et al., 2008). We used the Aerosol Optical depth at 550 nm for both ocean and land
817 product derived from eight-day average of global 1°x 1° gridded daily level-3 products from
818 MODIS/Aqua (MYD08_E3 Collection 5.1). MODIS AOD are derived using algorithms
819 detailed in Remer et al. (2005). Over oceans, MODIS AOD (τ) uncertainties have been shown
820 to be about $\pm (0.03 + 0.05\tau)$, over land retrieval uncertainties are generally $\pm(0.05 + 0.15\tau)$
821 (Remer et al., 2008). It is important to note that we had to use the eight-day average AOD

[product because the daily files had too much missing data due to the presence of clouds in the Vanuatu region.](#)

2.3 Model description and simulations

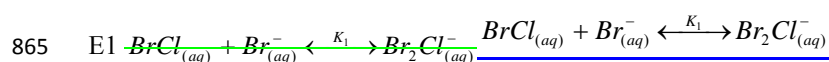
We use the CCATT-BRAMS (Coupled Chemistry Aerosol-Tracer Transport model to the Brazilian developments on the Regional Atmospheric Modeling System, version 4.3) non-hydrostatic regional atmospheric chemistry model (described in detail in Longo et al., 2013). It is based on the Regional Atmospheric Modeling System (RAMS) developed by University of Colorado for a range of applications: from large eddy simulations in the planetary boundary layer to operational weather forecasting and climate studies (Walko et al., 2000). BRAMS builds upon RAMS and includes modifications and new features to improve the model performances within the tropics (Freitas et al., 2009). The parameterizations of physical processes such as surface-air exchanges, turbulence, convection, radiation and cloud microphysics are described in Freitas et al. (2009) and in Longo et al. (2013). BRAMS is coupled on-line to CCATT that enables transport, chemical evolution, emission and deposition of chemical and aerosol species (Longo et al., 2013). Note that when BRAMS and CCATT are coupled, as in the present study, the prognostic chemical fields, O₃, N₂O, CO₂, CH₄ are used in the radiation scheme. The model has already been used to study regional air pollution, for instance: the South America regional smoke plume (Rosario et al., 2013) and ozone production and transport over the Amazon Basin (Bela et al., 2015). It has also been used to assess the transport of tropospheric tracers by tropical convection (Arteta, 2009a, b) and for understanding the budget of bromoform (Marécal et al., 2012).

The CCATT model is described in detail by Longo et al. (2013). Here we focus on the particular settings of the model we used and the changes we made for the study.

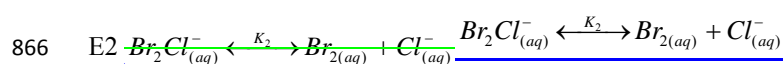
2.3.1 Model Chemistry

846 Within the CCATT model, we use the RACM chemistry scheme (Regional Atmospheric
 847 chemistry Mechanism, Stockwell et al., 1997) including 88 species and 237 chemical
 848 reactions and designed to study tropospheric chemistry from urban to remote conditions.
 849 Photolysis rates are calculated on-line during the simulation to take into account the presence
 850 of aerosols and clouds using Fast-TUV (Tropospheric ultraviolet and visible radiation model,
 851 Tie et al., 2003; Longo et al., 2013). The sulfur scheme includes gas-phase oxidation, and dry
 852 and wet deposition, but not aqueous-phase oxidation. In order to simulate halogen chemistry
 853 in volcanic plumes, we have added to the chemical scheme 16 halogen species and 54
 854 reactions including photolysis, gas phase and heterogeneous reactions. The gas phase constant
 855 rates and photolysis cross-sections are from JPL (Sander et al., 2006) and IUPAC (Atkinson
 856 et al. 2007). The heterogeneous reactions include the hydrolysis of BrONO₂ and the reaction
 857 of HOBr + X⁻_(aq) + H⁺_(aq) where X = Br or Cl on sulfate aerosol. They are treated here with
 858 reactive uptake formulation (Table 1) with constant uptake coefficient. Ongoing
 859 developments are being made to prescribe a variable reactive uptake coefficient for HOBr as
 860 function of the underlying gas-aerosol reaction kinetics, building on a recent re-
 861 evaluation (Roberts et al., 2014b).

862 For the heterogeneous reaction of HOBr_(g) with X⁻_(aq) where X = Br or Cl, there is a
 863 subsequent inter-conversion between the products Br₂ and BrCl within the aerosols, based on
 864 the equilibria (Wang et al., 1994):



Code de champ modifié



Code de champ modifié

As a result, the relative amount of Br₂ and BrCl produced and released into the atmosphere depends on the equilibrium established by these two reactions. The Br₂/BrCl ratio is given by E3 (derived from equilibria of Wang et al., 1994):

$$E3 \quad \frac{[Br_{2(aq)}]}{[BrCl_{(aq)}]} = \frac{K_1 [Br_{(aq)}^-]}{K_2 [Cl_{(aq)}^-]} \frac{[Br_{2(aq)}]}{[BrCl_{(aq)}]} = \frac{K_1 [Br_{(aq)}^-]}{K_2 [Cl_{(aq)}^-]}$$

Code de champ modifié

where the equilibrium constants of E1 and E2 are $K_1 = 1.8 \cdot 10^4 \text{ M}^{-1}$ and $K_2 = 1.3 \text{ M}^{-1}$ respectively and the amounts of [Br⁻] and [Cl⁻] in the aqueous phase are determined by the effective Henry's law constants (taken from Sander, 1999). We thus parameterize the reactive uptake coefficient of HOBr as two competing reactions (with Br⁻ and Cl⁻) and, on the basis of E3, apply a branching ratio to the constant rates of reactions as shown in Table 1. This approach is the same as that proposed by Grellier et al. (2014), and also similar to Roberts et al. (2014a) that showed competition between Br₂ and BrCl as products from HOBr reactive uptake, finding Br₂ is initially formed but BrCl becomes more prevalent once HBr becomes depleted. Note that heterogeneous reactions involving HOCl and ClONO₂ are slow compared to the reactions involving HOBr and BrONO₂ and are not taken into account in the model.

Mis en forme : Exposant

Mis en forme : Exposant

2.3.2 Sulfate aerosol surface density

In the model, sulphuric acid H₂SO₄ is a prognostic variable and assumed to be in totally in the aerosol phase. It is both directly emitted by the volcano (see section 2.3.3 for details) and produced by the reaction of SO₂ with OH in the gas phase. We assume to have only binary H₂SO₄-H₂O aerosol. Weight percent of H₂SO₄ in the aerosol (wt) and the density of aerosols (ρ_{aer}) are calculated with the analytical expression of Tabazadeh et al. (1997) depending on the temperature and relative humidity. Total volume of aerosol V_{aer} (per cm³) can then be calculated from H₂SO₄ concentrations, wt and ρ_{aer}. Few observations of volcanic aerosol size distribution exist, and none have been reported for Ambrym volcano plume. We assumed that

the aerosols size follows a log-normal distribution with a fixed median diameter ($D_{\text{median}} = 0.5$ μm) and a fixed geometric standard deviation ($\sigma = 1.8$). On this basis, the number of aerosol particles was deduced from V_{aer} , D_{median} and σ and the total aerosol surface densities (cm^2/cm^3) was then calculated (further details on lognormal aerosol distributions can be found in Seinfeld and Pandis, 2006). Here, the resulting surface area distribution (Figure 4s) has a surface median diameter of 1 μm and a maximum surface area of 7000 $\mu\text{m}^2/\text{cm}^3$ in the near-downwind plume ~~and will be discussed in the results section.~~

. This maximum value corresponds to a surface of $7 \times 10^{-11} \mu\text{m}^2/\text{molec. SO}_2^{-1}$, a value that lies in the range of order (10^{-11} - $10^{-10} \mu\text{m}^2/\text{molec. SO}_2^{-1}$) studied by Roberts et al. (2014a). It is also broadly consistent with a recent estimate of aerosol surface area (relative to SO_2) made for Mt Etna (Roberts et al., 2016). Ongoing developments are being made to improve the volcanic aerosol representation to include two modes with diameter varying with hygroscopy, based on recent observations (Roberts et al., 2015).

Mis en forme : Espace Après : 0 pt

2.3.3 Emissions:

To generate the emissions, we have used the preprocessor PREP_CHEM_SRC (version 4.3) code described in detailed in Freitas et al. (2011). Anthropogenic emissions were prescribed using the RETRO (REanalysis of the TROposhperic chemical composition) global database (Schultz et al., 2007). Fire emissions were estimated using the Global Fire Emissions Database (GFEDv2) with $1^\circ \times 1^\circ$ spatial resolution and a 8-day temporal resolution (van der Werf et al., 2006). Biogenic emissions were provided by a monthly mean climatology for the year 2000 produced with the MEGAN (Model of Emissions of Gases and Aerosols from Nature; ~~—~~) database (Guenther et al., 2006) ~~database.~~). Details on the treatment of volcanic emissions and its modification for this study are given in the following.

2.3.3.1 SO₂ emissions

In CCATT-BRAMS, volcanic SO₂ emission rates are prescribed using the AEROCOM (Aerosol Comparisons between Observation and Models) database (Diehl et al. 2012; Freitas et al., 2011). This database includes volcanoes listed in the Smithsonian Institution's Global Volcanism Program database (GVP) (~~Simkin and Siebert, 2002~~ [et al.: 2010](#)). Their emissions rates are assigned depending on their eruptive state (pre-eruptive, intra-eruptive, post-eruptive and extra-eruptive degassing), on their Volcanic Explosive Index (VEI) in case of eruption, and on additional information from TOMS (Total Ozone Mapping Spectrometer), OMI instruments and COSPEC (Correlation spectrometer) measurements) when available (Diehl et al., 2012).

Here, we replaced the values from the AEROCOM database for volcanoes of the Vanuatu Arc by more relevant information, when they were available. In particular, SO₂ emission rate for Ambrym (18.8 kt/day) is reported by Bani et al. (2009, 2012), using DOAS measurements (described in section 2.2.1) in conjunction with wind-speed estimates. The error on this source is about ± 20 % according to Bani et al. (2009).

SO₂ emissions rates of the most important volcanoes of the Vanuatu Arc in January 2005 are summarized in Table 2. Note that the Bagana volcano (6.140°S, 155.195°E, alt=1750 m) in Papua New Guinea was also in activity for the period of the simulation, with an emission of 3.3 kt/day of SO₂ according to the AEROCOM database.

2.3.3.2 HBr and HCl emissions

HBr and HCl emission rates are derived from the measurements of HBr, HCl and SO₂ average fluxes reported for Ambrym by Allard et al. (2009). These average fluxes were based on airborne DOAS (to determine SO₂ flux) combined with gas ratios (to SO₂) calculated from crater-rim deployments of filter-pack samplers (for HBr, HCl, HF ~~and~~ with SO₂) and Multi-Gas sensors (for CO₂, H₂O ~~and~~ with SO₂), and are representative of a mean volcanic

Mis en forme : Police : Calibri, 11 pt

Code de champ modifié

emission of Ambrym (Allard, personal communication). We did not use directly the HBr and HCl measurements but instead derived the HBr/SO₂ and HCl/SO₂ mass ratios ($8.75 \cdot 10^{-4}$ and 0.1, respectively) from the reported fluxes and applied them to our January 2005 SO₂ emission rate value to estimate the HBr and HCl emissions specifically for this date. Indeed, volcanic emission fluxes can vary with time. Allard et al. (2009) ~~mean~~-reported mean SO₂ emission rate for instance totals 8.8 kt/day, about two times smaller than the SO₂ emission rate reported during the extreme passive degassing event of 18.8 kt/day, but in closer agreement ~~though~~ with the estimate by Bani et al. (2012) of Ambrym mean activity of 5.4 kt/day for the period 2004-2009. The calculation yields HCl and HBr emissions of 1.9 kt/day and 16.5 t/day. Of note, the HBr/SO₂ and HCl/SO₂ mass ratios are close to (for HBr/SO₂ perhaps somewhat higher-~~than~~) mean estimates for volcanic degassing as reported by Pyle and Mather (2009), but due to the high Ambrym SO₂ flux they yield very high volcanic halogen fluxes. By comparison, the Br flux from Mt Etna is reported as only 0.7 kt/yr (Aiuppa et al., 2005) i.e. 1.89 t/day, almost 10 times smaller. Note also that HF emissions were not considered in this study: whilst deposition impacts from HF around Ambrym can be severe (Allibone et al. 2010), HF does not contribute to reactive halogen cycling in the atmosphere (prevented by the strong H-F bond).

2.3.3.3 Sulfate emissions

We assume that 1% of the sulphur (= SO₂ + H₂SO₄ here) is emitted as H₂SO₄ aerosol based on reported observations from several filter-pack studies at different volcanoes worldwide (e.g., Mather et al., 2003, Von Glasow et al., 2009 and references therein).

2.3.3.4 Initialisation with output from HSC Chemistry thermodynamic model

As mentioned earlier (see Section 1), the mixing of volcanic gas with ambient air at the vent leads to high temperature oxidative dissociation processes and hence to the formation of radical species. To take into account this high temperature chemistry, the thermodynamic

model HSC Chemistry (Roine, 2007) was applied to simulate the equilibrium chemical composition of the volcanic gas-air mixture assuming a 98:2 volcanic gas:atmospheric gas composition. This approach follows that of previous 1D model studies (Bobrowski et al., 2007, Roberts et al., 2009, Von Glasow 2010, Kelly et al., 2013, Roberts et al., 2014a, Surl et al., 2015). The model temperature was based on mixing an atmospheric temperature of 20 °C (consistent with that predicted by the CCATT-BRAMS model) and the magmatic degassing temperature of 1125 °C estimated by Sheehan and Barclay (2015). This was based on calculation of crystallisation temperatures of mineral phases in scoria samples collected from Ambrym in 2005, following models of Putirka (2008). The HSC Chemistry model input composition, shown in Table 3, is a 98:2 mixture of magmatic gases (with composition based on Allard et al., 2009), and atmospheric gases (78% N₂, 21% O₂, 1% Ar). Roberts et al. (2014a) identifies key new species in the HSC Chemistry output as Br, Cl, OH and NO. Fluxes of these species were calculated from their ratio to sulphur in the HSC Chemistry output, and by scaling with the (prescribed) SO₂ flux in the CCATT-BRAMS model. Due to uncertainty in volcanic NO_x emissions (see discussions of Martin et al., 2012; Roberts et al., 2014a; Surl et al., 2015). Finally, HSC Chemistry ~~output~~ outputs both with and without NO_x were used to initialise CCATT-BRAMS (Simulations S1_HighT and S1_HighT_noNO_x). Note that the HSC output also contains SO₃, which is the precursor to volcanic sulfate. However, as mentioned above, in this study the volcanic sulfate emission was instead fixed to 1% (by mole) of sulfur in all runs. All the emissions for the different simulations are summarized in Table 4.

2.3.3.5 Plume height

The information on plume heights is from AEROCOM database and from Bani et al. (2012). They give respectively plume heights of 1373 m and of 2000 m (in our study, all the altitudes are above sea level unless otherwise mentioned). Note that the mean altitude of both crater

rims is about 1000 m. Bani et al. (2012) report an altitude of the plume of 2000 m for the degassing event of 12th of January 2005 that was estimated visually. For the other periods, their estimation of the altitude varies between 700 m (i.e. below the craters) and 2000 m. For the case study of the degassing event of January 2005, it was not clear to us from videos and pictures that the plume altitude was about 2000 m. As a result, we performed a sensitivity study on the plume height (see Supplementary Material). In a first simulation, emissions are injected in the model box vertically above the volcano that includes the 1373 m altitude point. This model box is not the same in each grid, as the topography depends on the grid resolution. As a result, its depth varies between about 100-200 m. In a second simulation, emissions are injected higher up in the box containing the 2000 m altitude, whose depth varies between about 200-300m. As shown later, we performed an additional sensitivity analysis, where the emissions are this time spread over two vertically adjacent grid boxes (section 3.3.1). The depth of the plume in the model this time is about 300 m to 400 m. Figure 1 shows the distribution of volcanic emissions in the vertical prescribed in the model for the different sensitivity simulations.

2.3.4 Model general set-up and simulations

In our study, the primary horizontal resolution is $50 \text{ km} \times 50 \text{ km}$ with 44 vertical levels from the ground to 27 km. Three nested grids ($10 \text{ km} \times 10 \text{ km}$, $2 \text{ km} \times 2 \text{ km}$ and $0.5 \text{ km} \times 0.5 \text{ km}$) was also added. Model domain and grids are shown in Figure 2. Horizontal winds, geopotential height, air temperature and water vapor mixing ratios from ECMWF analysis (with a $0.5^\circ \times 0.5^\circ$ resolution) are used to initialize and nudge the model –using a four dimensional data assimilation (4DDA) technique with a relaxation time constant ranging from 30 min at the lateral boundaries to 6 hours at the center of the domain. Initial and boundary conditions for concentrations of the chemical species were provided by 6-hourly

1014 output from the global chemical transport model MOCAGE (Josse et al., 2004) with a
1015 resolution of $1^\circ \times 1^\circ$.

1016 In the following, we describe the different simulations performed in this study. All the
1017 simulations start the 1st of January 2005 00:00 UTC with the larger grid only. As this was an
1018 extreme degassing event of long duration (several months) rather than an episodic eruption,
1019 the model initialization from 1st January 2005 already includes the Ambrym emissions. Due
1020 to computing limitations, the 3 nested grids are only added the 11th of January 2005 00:00
1021 UTC with the initial conditions given by the corresponding simulation with one grid. The
1022 different simulations differ in terms of the strength of the emissions, the nature of the emitted
1023 compounds and the repartition of the emissions in the vertical. They are summarized below,
1024 as well as in Table 4 and Figure 1:

- 1025 - S1 includes the standard volcanic emissions (SO_2 , H_2SO_4 , HCl , HBr).
- 1026 - S1_HighT includes emissions (SO_2 , H_2SO_4 , HCl , HBr , OH , NO , Cl , Br) derived from an
1027 HSC Chemistry simulation described in section 2.3.4.4 and in Table 3.
- 1028 - S0 has the same emissions as S1_HighT except that emissions from Ambrym volcano have
1029 been turned off.
- 1030 - S1_HighT_alt simulation is exactly the same as S1_HighT except that the height of plume is
1031 fixed to 2000m.
- 1032 - S1_HighT_width is exactly the same than S1_HighT except that the plume of Ambrym
1033 spans two grid boxes (in the vertical) instead of one.
- 1034 - S1_HighT_noNOx simulation is exactly the same than S1_HighT except that emissions of
1035 NO have been turned off.
- 1036 - S1_nohal has the same emissions as S1_HighT except that Ambrym volcano includes only
1037 SO_2 emissions.

1038 - S1_nohal2 has the same emissions as S1_HighT except that Ambrym volcano includes only
1039 SO₂ emissions and the same emissions of OH than S1_HighT.
1040 - S1_HighT_surf is exactly the same than S1_HighT except area surface density was
1041 increased by a factor of 10.
1042 In the next section, we evaluate the performances of the model CCATT-BRAMS to simulate
1043 near downwind volcanic plume chemistry for the Ambrym extreme passive degassing of 12th
1044 January 2005 ~~in regard of the previous work and~~ using the airborne DOAS observations of
1045 SO₂ and BrO columns [and in the context of previous work](#).
1046

1047 **3. Analysis of the modeled volcanic chemistry in the near downwind plume**

1048 **3.1 Evaluation of the modeled SO₂ and BrO columns amounts in the near downwind** 1049 **plume**

1050 Figure 3 shows the SO₂ columns amounts observed during 4 traverses of the near downwind
1051 Ambrym plume (between 15 to 40 km of the vent) on 12th January 2005 between 05:00 and
1052 06:00 UTC (Bani et al. 2009; 2012) and the corresponding SO₂ columns amounts simulated
1053 by the model for the S1 (i.e. including the standard emission) and S1_HighT (i.e. initialized
1054 with the output of the HSC Chemistry model as described in Section 2.3.3.4) on the grid 0.5
1055 km × 0.5 km (see section 2.3.4 for the description of the simulations). Statistical quantities
1056 (mean, RMS, correlation) were calculated to compare more quantitatively observations and
1057 simulations (Table 5). Note that sensitivity studies to the height of the plume and the vertical
1058 extent of the plume will be discussed further in section 3.3.

1059 **3.1.1 SO₂ columns**

1060 Observations show that SO₂ columns decrease with distance from the vent and exhibit a
1061 bimodal distribution across the plume. Each mode is attributed by Bani et al. (2009) to the

individual plume of the two degassing craters Benbow and Marum that are situated 3km apart. Figure 3 shows that the model captures relatively well the magnitude of the SO₂ columns along and across the plume for the S1 and S1_HighT simulations. The mean difference between observations and simulations is lower than 2% (relatively to the mean of the observation) and the correlation coefficient is about 0.6 (Table 5). However, we can note that the influence of the 2 craters Benbow and Marum is not seen as clearly as in the observations. This suggests a limitation linked to the model resolution, even though the model resolution for the particular grid shown is 500 m × 500 m. We can also note that the simulated plume tends to be slightly tilted eastward compared to the observations -in particular for the transects at 20 km and 21 km (not shown) from the vent but to a lesser extent for the transect at 40 km-. This is the reason for the relatively high RMS values (about 50 % of the mean SO₂, see Table 5) but it does not affect the bias (2%).

Previous work at volcanoes elsewhere (e.g., Bobrowski et al., 2007) reported that the observed SO₂ variations in the near downwind plume are almost exclusively due to plume dilution. As a test, we have included in our simulation an SO₂ “tracer” whose emission and deposition are the same as for SO₂ but whose chemical loss is equal to zero. We find that the difference between the SO₂ columns field and the SO₂ tracer columns field at a distance of 40 km from the vent is less than 0.5 % (not shown), confirming that the SO₂ decrease in the model with distance from the vent in Figure 3 is mostly due to plume dilution. Therefore, we can conclude from the comparison in Figure 3 that the direction of the plume as well as its dilution are reasonably well simulated by the model in the simulations S1 and S1_HighT. It is important to note that we cannot conclude here on the strength of the Ambrym SO₂ source. Indeed, our rationale would be circular as we have used in our model the SO₂ source strength (described in Section 2.3.3.1 and Table 2) which Bani et al. (2009, 2012) derived from the same DOAS data (combined with winds estimates) used here for the model evaluation. Note

also that we performed a simulation S1_HighT_alt, similar ~~than~~^{to} S1_HighT except that the plume height was 2000 m as reported by Bani et al. (2012). We find that the simulation S1_HighT_alt (see supplementary material section 1 as well as Figures 1S and 2S for more detail) underestimates the observations by 44 % for SO₂ (compared to 2% for S1_HighT). The correlation between simulated and observed SO₂ is also reduced, 0.37 (compared to 0.61 for S1_HSC). Given better agreement between the model and observations at the lower injection altitude estimate of ~1400 m, this injection height of S1_HighT was used in the following.

1095

1096 3.1.2 BrO columns

In Figure 4, the same comparison as for Figure 3 is presented for BrO columns amounts. BrO columns, as those of SO₂, decline between 15 and 40 km from a mean of 9.8×10^{14} molecule/cm² to a mean 3.2×10^{14} molecule/cm². Values as high of 1.8×10^{15} molecule/cm² at 15 km were reported by Bani et al. (2009). Note that these values are particularly high compared to other BrO column observations at volcanoes elsewhere for which maximal values lie between ~~1×10^{14}~~ ^{1×10^{14}} molecule/cm² to ~~1×10^{15}~~ ^{1×10^{15}} molecule/cm² (Boichu et al., 2011). Note also that the influences of the two crater sources (Benbow and Marum) are still visible in the BrO data as two distinct peaks.

In the standard simulation, the trend in BrO with distance from the vent is reversed compared to the observations (also shown by the negative correlation coefficient of Table 5 of -0.21). At 15-20 km downwind from the vents where observed BrO columns are highest, the model (S1) underestimates the mean BrO columns by a factor of 10. Overall, the mean difference between BrO columns observed and those simulated in S1 is about 80 % (Table 5). ~~An improved agreement between model and observations is shown for~~^{For} the simulation initialized with ~~HighT (as seen in Figure 4): the mean bias between S1_HighT and~~

1112 ~~observations is reduced and is about 40%. In addition~~[HSC Chemistry model](#), the trend in BrO
1113 with distance from the crater is in better agreement with the observations (Figure 4 and
1114 correlation coefficient of Table 5 of 0.6). [An improved overall agreement between model and
1115 observations is also found \(as seen in Figure 4 and Table 5\): the mean bias between observed
1116 and simulated BrO columns is about 40% \(relative to the mean observations\). It is important
1117 to note that the bias is more pronounced near source: it varies from 60 % for the transect at
1118 15 km to 14 % for the one at 40 km of the vents.](#)

1119 Figure 5 shows the evolution of BrO/SO₂ with distance from the vent derived from the
1120 observations and from the simulations presented in Figure 3 and 4. Because SO₂ can be
1121 considered as a passive tracer over short timescales, any increase or decrease in BrO/SO₂
1122 implies respectively a production or a destruction of BrO. Measurements suggest that BrO
1123 formation has occurred and has reached its maximal amount between 0 and 17 km of the vent.
1124 Further downwind, between 17 km and 40 km, measurements predict a destruction of BrO. In
1125 the simulation initialized with the HSC Chemistry model, the trend in BrO/SO₂ is close to that
1126 observed. The formation of BrO reaches a maximum around 17 km with a plateau between 17
1127 and 21 km and is destroyed between 20-21 and 40 km. In contrast, in the case of the standard
1128 simulation S1, BrO builds up between 15 and 40 km. Overall, we conclude that BrO
1129 formation is too slow in the standard simulation compared to the observations. On the
1130 contrary, the kinetics of BrO formation predicted in the simulation initialized with HSC
1131 Chemistry model ~~is~~ in good agreement with the observations. This confirms previous [1D
1132 model](#) work that showed the need for radicals to “kick off” the chemistry i.e. accelerate the
1133 onset of the chemistry (e.g., Bobrowski et al., 2007; Roberts et al., 2009). In addition, Figure
1134 5 shows that, for each transect, the variability of BrO-/SO₂ ratios in the observations and in
1135 the S1_HighT simulation have a similar magnitude. In particular, we find that for each
1136 transect the model simulates the highest value of the BrO/SO₂ ratio at the edges of the plume

as shown in the observations, i.e. for lowest values of SO₂ columns. This result is again consistent with previous work (e.g., Bobrowski et al., 2007; Von Glasow [et al. 2009](#); [von Glasow](#), 2010; Roberts et al., 2014a). At the edges of the plume, more mixing with entrained background air occurs. This leads to higher ozone concentrations and favors BrO— ([see section 2.1.2](#)). In general, the trends in BrO/SO₂ with distance downwind and between core and plume edge reflect the net impact of a dynamic chemistry involving many reactive bromine chemistry species. In the following section, we analyze in more detail the simulation of volcanic plume chemistry.

3.2 Simulated plume chemistry

Figure 6 shows distance-pressure cross ~~section~~[sections](#) of SO₂, OH, HBr, BrO, O₃ and NO_x mixing ratios in the plume of the standard simulation for the 12th of January 2005 at 6 UT (time of the DOAS measurements) in the grid 2 km ~~×~~ 2 km. This grid allows us to visualize the results as far as 200 km downwind. Figure 7 shows the Br speciation among the bromine species along the plume (in the core and at the edges) for the same simulation in the same grid and at the same time. Figure 6 shows that OH is totally depleted in the core of the plume in the simulation. This is due to the elevated concentrations of SO₂ as well as being a consequence of the halogen chemistry (see section 4.4), and mirrors findings from previous ~~volcano-plume~~[1D model](#) studies (e.g., Roberts et al., 2009, 14a; Von Glasow, 2010). However, as noted before, the decrease of SO₂ along the plume as far as 200 km is mainly due to dilution of the plume. Figures 6 and 7 show that HBr is converted into reactive bromine in the volcanic plume, as expected. However, at about 50 km of the vent, only 20% of this conversion had occurred (80 % HBr remains). Indeed, the chemical cycle responsible for HBr conversion is autocatalytic so it needs reactive bromine to be initiated. In the standard simulation, the onset of BrO formation is slow because reactive bromine is initially formed by

1162 the reaction of HBr with OH, which is slow because OH is depleted. In Figure 6, the
 1163 enhancement of BrO (and of Br₂ in ~~the~~ Figure 7) as well as the depletion of O₃, NO_x and HO_x
 1164 (not shown) confirm that the autocatalytic cycle responsible for HBr conversion to reactive
 1165 bromine is ongoing in the simulations- [\(see section 2.1.2\)](#). Very quickly, in the core of the
 1166 plume, BrO becomes the dominant species after HBr. Its mixing ratio increases with distance
 1167 from the vent reaching a maximum of 120 pptv at about 70 km (Figure 6) equivalent to 20%
 1168 of the total bromine (Figure 7). The depletion of ozone reaches its maximum of 15 ppbv loss
 1169 (100%) at 70 km, corresponding to the maximum of BrO. Further downwind, Br is the
 1170 dominant species because O₃, HO_x and NO_x are depleted. In contrast, at the edges of the
 1171 plume, BrO is still increasing and dominates because more ozone is available than in the core
 1172 of the plume enabling its formation from Br- [\(R3\)](#). Further downwind at the edges of the
 1173 plume, the formation of BrO slows but does not stop (as shown by the non-zero Br₂ and BrCl
 1174 fraction) as the plume disperses and dilutes the volcanic aerosol. A dynamic equilibrium is
 1175 established between BrO, Br and HOBr. We can note that the BrO mixing ratio remains as
 1176 high as 60 pptv at the edge of plume around 200 km downwind (Figure 6).
 1177 As expected, in the simulation initialized with HSC Chemistry model, the conversion of HBr
 1178 into reactive bromine is accelerated by the presence of the radical species (Figure 8 and 9).
 1179 Indeed, the HBr fraction is only 20 % at 25 km from the vent and is almost zero around 30 km
 1180 downwind at the edge of the plume. Once HBr becomes depleted, a peak of BrCl is observed
 1181 because the aqueous phase equilibria between BrCl and Br₂ favor BrCl instead of Br₂. Figure
 1182 8 shows that BrO reaches its maximum earlier, around 15-20 km downwind, than for the
 1183 standard simulation (70 km), at a distance where the plume is more concentrated. As a result,
 1184 the maximum of BrO mixing ratios is higher (around 240-260 pptv) than for the standard
 1185 simulation. Ozone is also entirely depleted in this simulation, it reaches 15 ppbv loss (100 %)
 1186 around 15 km. In the core of the downwind plume Br becomes the dominant species (up to

1187 80 % of Br₂, Figure 9) due to this total ozone depletion with ongoing ozone loss processes
1188 exceeding any source from entrainment of (ozone-containing) background air into the plume
1189 core. HBr can reform by the reaction of Br with HCHO for instance because of the high
1190 concentrations of Br in the core of the plume. Further downwind, HBr is then slightly
1191 reconverted into BrO, likely because a somewhat enhanced entrainment of ambient air occurs.
1192 At the edges of the plume, the chemical cycles are not limited by lack of (background)
1193 oxidants. As a result, HBr can be fully consumed and BrO is the dominant species. Further
1194 downwind, the formation of ~~reactive~~ ongoing reactive halogen chemistry results in a dynamic
1195 equilibrium being established between BrO, Br and HOBr. ~~To conclude, we find that the~~
1196 ~~formation of reactive bromine species is faster in the S1_HighT simulation than in S1. This~~
1197 ~~leads to higher BrO concentrations in near downwind plume and hence to a better comparison~~
1198 ~~with DOAS data. However, we~~ We can also note that even further downwind (approximately
1199 from 150 km ~~off~~from the vent), there is no significant difference between S1 and S1_HighT in
1200 terms of absolute concentration of the bromine species and in terms of partitioning among the
1201 bromine species.

Mis en forme : Couleur de police :
Noir

1202 To conclude, the kinetics of BrO formation predicted in the simulation initialized with HSC
1203 Chemistry model is in good agreement with the observations. This leads to higher BrO
1204 concentrations in near downwind plume and hence to a better comparison with DOAS data.

Mis en forme : Espace Après : 10 pt

1205 Despite the better comparison between DOAS and S1_HighT, ~~the maximal model still~~
1206 ~~underestimates by 60 % the~~ BrO columns ~~($5.7 \cdot 10^{14}$ molecules/cm²) in the S1_HighT~~
1207 ~~simulation are still three times lower than the maximal values observed in the near-source~~
1208 plume (at 15 km from the vents). We find that it is due to the ozone depletion in the core of
1209 the plume that limits the formation of BrO from Br. In strong (i.e. near-source and under high
1210 emissions) volcanic plumes, gas-phase cycling between Br and BrO (reactions, 3, 4a and 4b)

Mis en forme : Couleur de police :
Automatique

1211 is particularly intense. As a consequence, in the core of the plume where the mixing with
1212 background ozone is limited, ozone is totally depleted. This lack of ozone limits the
1213 partitioning of BrO from Br and hence BrO concentrations.

Mis en forme : Couleur de police :
Noir

1214 ~~In the following~~As presented in section 2.3, we ~~investigate the sensitivity~~had to make some
1215 assumptions in our study because of the model results to the depth of the plume in the model
1216 ~~initialization, the presence of NO_x in the emissions and the surface aerosol area density. In~~
1217 ~~particular~~lack of information to constrain the model or technical limitations. In the next

Mis en forme : Couleur de police :
Noir

Mis en forme : Couleur de police :
Noir

1218 section, we test whether the uncertainties in these variablesthe representation of some of the
1219 crucial processes could affect the model results and explain the discrepancies found between
1220 simulations and observations for the closest transects (~15-20 km) from the vents. More
1221 specifically, we focus on the depth of the plume that controls the degree of mixing between
1222 emissions and background air, the formation of NO_x by the high temperature chemistry and
1223 the surface aerosol area that can affect the in-plume chemistry.

Mis en forme : Couleur de police :
Noir

Mis en forme : Couleur de police :
Noir

Mis en forme : Non Surlignage

1224

1225 3.3 Sensitivity studies

1226 3.3.1 Vertical depth of the plume.

1227 A suggested in section 3.2, BrO formation appears to be limited by ozone concentrations in
1228 the simulation S1_HighT. However, values of background ozone in the model seem in good
1229 agreement with ozone climatology (e.g., Logan et al., 1999) that indicates ozone mixing ratios
1230 of 15-20 ppbv below 800 hPa in the Pacific region. Here in an attempt to avoid the limitation
1231 of BrO formation due to lack of ozone, we have ~~spread~~increased the degree of the mixing
1232 between the emissions and the background air in the vertical. Practically, we have artificially
1233 increased the vertical depth of the plume by spreading out the emissions over two vertically
1234 adjacent levels (see Figure 1). More specifically, in the simulation S1_HighT_width, the

emissions were distributed equally between the vertical grid box of the S1_HighT simulation and the one just above. ~~In this way~~ As a result, the Br molecules are exposed to roughly twice as many ozone molecules. ~~However,~~ Note that we did not change the degree of mixing in the horizontal because Figure 3, showing the comparison of SO₂ columns distribution across the plume, seems to indicate that the width of the plume at different distances from the vents is reasonably well simulated by the model.

We find ~~again~~ that the comparison with DOAS for SO₂ does not improve (mean bias of 17 % and a correlation of 0.55, Figure 1S). Concerning BrO, our results are very similar to those obtained with S1_HighT (slightly worse with mean bias of 43% and with a correlation coefficient of 0.54, Figure 2S). ~~This~~ The weak impact of this sensitivity study can be explained by the fact that the vertical diffusion in the model has already dispersed very quickly the emissions through several vertical levels ~~(in S1_HighT)~~. Thus, BrO formation is already limited by ozone in the upper level where the emission was additionally injected in S1_HighT_width. ~~However, when spreading~~ As a result, we have tried different combinations to spread out the emissions over more than 2 levels in the vertical between the level of injection of S1_HighT (~1400 m) and the level of injection of S1_HighT_alt (~2000 m) (see Figure1). But, the wind direction changes with the altitude between these two levels in our simulations. Therefore, the comparison ~~between~~ of SO₂ columns ~~simulated and observed becomes worse (not shown) and~~ distribution across the plume, that was fairly good for S1_HighT, worsens in these model runs and tends to become very similar to the one obtained with S1_HighT_alt: (see Figure 1s).

Mis en forme : Indice

3.3.2 Formation of NO_x by high temperature chemistry

Mis en forme : Police :Gras

There are numerous uncertainties concerning the high temperature chemistry taking place in the mixture of volcanic gases and ambient air at the vent (Martin et al., 2009; 2012). In particular, models used to calculate this chemistry assume thermodynamic equilibrium.

However, Martin et al. (2012) calculated that the thermal N_2 fixation is too slow for equilibrium to be attained at volcanic vents. Hence, the production of NO_x by the HSC model could be overestimated. Conversely, volcanic NO_x production is suggested by several observations of NO , NO_2 , HNO_3 , HO_2NO_2 in the near-source plume (e.g., Mather et al. 2004; Oppenheimer et al., 2010; Martin et al., 2012, Voigt et al., 2014), with NO_x to HNO_3 conversion pathway proposed by Roberts et al. (2009, 2014a). In the case of Ambrym, no information is available on the absence or presence of volcanic NO_x , nor other reactive nitrogen species in the plume. We performed a simulation (S1_HighT_no NO_x) where NO_x from the high-temperature initialization was not included while keeping constant the emissions of the other radicals (i.e. OH, Cl, Br) from HSC Chemistry. In this case, the SO_2 field is exactly the same as in S1_HighT (Figure 1S). The comparison between BrO in S1_HighT_no NO_x and the observations (Figure 2S) is very close to what is obtained for S1_HighT (mean model observation difference is about 44% and the correlation is about 0.63). Figure 3S gives some explanation for this. It shows that the kinetics of HBr conversion in S1_HighT_no NO_x is similar to that in S1_HighT in the first 10-15 km from the vent and it is much slower after 15 km. This suggests that ~~other radicals from the high-temperature initialization than NO_x are~~ NO_x emissions are not crucial to kick off the plume chemistry initially ~~and but~~ that ~~afterwards NO_x emissions become important~~ they are responsible for the decline of HBr further downwind after 15 km. This delayed role of the NO_x radicals was also found in 1D model study presented by Roberts et al. (2009) (see their figure 4). In our case, this is further confirmed by Figure 8 ~~when~~ where it can be seen that NO_x depletion in S1_HighT starts after 10-15 km. The role of NO_x is linked to the formation of $BrONO_2$ from BrO and NO_2 followed by its rapid hydrolysis on volcanic sulfate aerosol that acts to convert BrO into HOBr and that can then undergo another heterogeneous chemical cycle to release reactive bromine from HBr ($Br_{(aq)}^-$). Without NO_x , this conversion of BrO into

Mis en forme : Indice

Mis en forme : Indice

HOBr ~~can come only from~~ depends on the presence of HO₂ via the reaction of BrO with HO₂.
 Note also that due to the slower decrease of HBr in S1_HighT_noNOX after 10-15 km, no
 BrCl peak is visible in Figure 3S in the near downwind in contrast to Figure 9 for the
 S1_HighT simulation. To conclude, the difference in BrO kinetics in S1_HighT and
 S1_HighT_noNOx is mostly visible after 10-15 km from the vent. Hence, it does not impact
 the initial near-downwind rise in BrO. This contrasts with the model studies of Von Glasow
 (2010) and Surl et al. (2015) for Mt Etna who suggested a volcanic NO_x emission acts to
 lower plume BrO due to the formation of BrNO₂ that persists in the plume. However, Roberts
 et al. (2014a) highlighted additional pathways for BrNO₂ removal enabling regeneration of
 BrO. Given uncertainties in the chemistry, BrNO₂ is not included in our study.
 To conclude, the simulations S1_HighT and S1_HighT_noNOx exhibit similar kinetics of
 BrO formation and also a similar magnitude in the BrO maximum. As a result, uncertainty in
 the presence of volcanic NO_x in the emission cannot explain the discrepancy between the
 model and reported downwind plume BrO. In addition, we can also note that the BrO and
 SO₂ columns measurements alone are not sufficient to fully constrain the parameter space of
 our modeling of volcanic plume chemistry. In particular, NO_x and HNO₃/nitrate should be
 measured in volcanic plumes to constrain the reactive nitrogen emission.

3.3.3 Sulfate aerosol surface density

~~In Figure 4S, Despite a broad agreement with previous estimates (see section 2.3.2), aerosol~~
~~surface density remains a source of uncertainty in our study our as we show do not have direct~~
~~measurements of aerosols for Ambrym. Therefore we have increased the simulated sulfate~~
~~aerosols aerosol surface density available for heterogeneous reactions. The maximum by a~~
~~factor 10, still keeping the value is $7 \times 10^3 \mu\text{m}^2/\text{cm}^3$ corresponding to a surface of 7×10^{11}~~
 ~~$\mu\text{m}^2/\text{molec. SO}_2^{+}$, a value that lies in the in the right range of order (10^{11} – 10^{10} $\mu\text{m}^2/\text{molec.}$~~
 ~~SO_2^{+}) studied by Roberts et al. (2014a). It is also broadly consistent with a recent estimate~~

Mis en forme : Espace Avant : 0 pt.
 Ne pas ajuster l'espace entre le texte
 latin et asiatique, Ne pas ajuster
 l'espace entre le texte et les nombres
 asiatiques

Mis en forme : Police : Non Gras

1310 ~~of~~ [section 2.3.2](#)), to test whether this uncertainty could explain the pronounced discrepancy on
1311 [BrO columns near-source](#). We would expect that an increased [aerosol surface area](#) ~~(relative to~~
1312 ~~SO₂) made for Mt Etna (Roberts et al., 2015). Here, we performed a sensitivity study by~~
1313 ~~increasing the sulfate aerosols surface density by a factor 10 (not shown).~~ [would increase the](#)
1314 [conversion of HBr into reactive bromine and hence the concentrations of BrO](#). Note, that this
1315 [sensitivity study is equivalent to increase the HOBr reactive uptake coefficient on sulfate](#)
1316 [aerosols, for which large uncertainties exist \(see Roberts et al., 2014a\), while keeping](#)
1317 [constant the aerosol surface area](#). We find that ~~it does not impact the value of near source~~
1318 ~~BrO/SO₂ consistent with our above finding that~~ [our sensitivity study impacts only very slightly](#)
1319 [the value of near-source BrO columns \(bias of 62 % compared to the bias of 60% for](#)
1320 [S1_HighT\)](#). Indeed, BrO is determined by the [partitioning with Br mainly by reactions R3,](#)
1321 [R4a and R4b in the concentrated plume](#). Because ~~ozone depletion is the limiting control on~~
1322 ~~BrO in near downwind Ambrym plume,~~ [quickly consumed, the formation of BrO is limited as](#)
1323 [discussed earlier](#). This is also in agreement with the sensitivity studies performed with the
1324 PlumeChem model (Roberts et al. 2014a) for Mt Etna where increasing the aerosols surface
1325 density ~~by a factor 10 increased only slightly the BrO/SO₂ ratio in the near downwind~~
1326 ~~plume.~~ [Note that we did not test the sensitivity of the model results to the strength of total](#)
1327 [bromine emissions. Increasing total bromine emissions would increase total bromine in the](#)
1328 [plume. But because of the ozone limitation, this would lead to a reduced fraction of BrO and](#)
1329 [increased fraction of Br. Finally, these two effects would compensate as found with a 1D](#)
1330 [model for the Nyiragongo's plume by Bobrowski et al. \(2015\). As a result, increasing total](#)
1331 [bromine emissions would not impact BrO columns. This compensation was also found by](#)
1332 [Roberts et al. \(2014\) with their 1D model when compared their “high” and “medium” total](#)
1333 [bromine scenarios](#).

1334

1335 To conclude, the uncertainties on plume depth, NO_x emissions, aerosol loading as well as
 1336 injection height cannot explain the discrepancy between the model and the reported near
 1337 source BrO. Instead, we find that BrO formation is ozone limited in our model runs. This is
 1338 also found in the model 1D runs of Bobrowski et al. (2015) of the Nyiragongo's plume, who
 1339 conclude that measurement of ozone should be a priority for next measurements campaigns.
 1340 More generally, BrO and SO₂ columns measurements are not sufficient to constrain the
 1341 modeling of volcanic plume chemistry as also highlighted in Bobrowski et al. (2015). It is
 1342 also important to note that the discrepancy between simulated and measured BrO columns
 1343 remains limited to the near downwind plume. Indeed, the modeled BrO columns agree within
 1344 14 % with the farthest observations (~40 km of the vents). As the result, this discrepancy does
 1345 not significantly impair the analysis of the regional impact of Ambrym presented below.

1346 **4 Regional impact of Ambrym volcanic emissions**

1347 **4.1 Evaluation of the plume simulation at the regional scale with OMI**

1348 Figure 10 shows SO₂ columns on 12th of January 2005 at 02:30 UT from OMI and the
 1349 corresponding SO₂ columns interpolated on the OMI grid from CCATT-BRAMS. The model
 1350 result is for the grid resolution of 10 km ~~*x~~ 10 km that is of similar size to the OMI data (13
 1351 km ~~*x~~ 24 km). ~~Figure 10 suggests that the direction of the plume is correctly simulated at the~~
 1352 ~~regional scale.~~ At this time of the year, the plumes from Marum and Benbow are generally
 1353 carried to the northwest by the trade winds. ~~In~~As shown, in Figure 10, on January 12th 2005,
 1354 they were carried to the south, because of the influence of the Cyclone Kerry, located around
 1355 1800 km southwest of Vanuatu (Bani et al., 2009). Figure 10 suggests that the direction of the
 1356 plume is correctly simulated at the regional scale. To quantify the degree of spatial matching
 1357 between modeled and observed SO₂ plumes, we have calculated the Figure of Merit in Space
 1358 (FMS) which is the ratio between the intersection of the observed and simulated plumes areas
 1359 and their union (Mosca et al., 1998). Using a threshold of 5×10^{16} molec. SO₂/cm² to define

Mis en forme : Espace Avant : 0 pt,
 Ne pas ajuster l'espace entre le texte
 latin et asiatique, Ne pas ajuster
 l'espace entre le texte et les nombres
 asiatiques

the Ambrym plume in both OMI and model fields, we find a FMS of 62% that suggests a fairly good spatial agreement between observed and modeled plumes. The difference between OMI and the model observed and simulated SO₂ columns distributions is mainly due to the plume width that is slightly larger in the model than in OMI (Figure 10). In addition, further downwind in the plume simulations than in OMI data (Figure 10). The magnitudes of the mean columns in both plumes match also fairly well: the mean difference is about 25 % (relative to the observations). This difference is due to the presence of some SO₂ enhancements in the plume in the OMI data that are not seen in OMI data but not in the simulations. Note that the truncated length of the SO₂ plume in the OMI data is related to the presence of clouds north east of New Caledonia. It is important to notice that the present comparison also shows that simulated SO₂ columns, when initialized with the Ambrym SO₂ source strength estimate derived from the DOAS observations by Bani et al. (2009) and (2012), agree within 25 % to the SO₂ columns detected by OMI.

Mis en forme : Anglais (Royaume-Uni)

4.2 Impact of Ambrym on sulfate, bromine and ozone at the regional scale

Our simulations include 4 grids. To study impacts of Ambrym at the regional scale, model outputs for the largest grid (see Figure 2), whose resolution is 50 km x 50 km, are analyzed. Because of computing limitations, we present only the impact for the 12th January 2005 after 11 days of spin-up.

4.2.1 Sulfate

The sulfate burden in the model domain due to Ambrym increases by 44% (i.e. 0.08 Tg of sulfate) value calculated as the mean difference in sulfate between S1_HighT and S0 for 12th January. The direct sulfate emission totals 3.34 Gg of sulfate since the beginning of the simulation. This means that at least 96 % ($\approx (80-3.34)/80 \times 100$) of the sulfate burden increase due to Ambrym results from the atmospheric oxidation of SO₂ from the volcano by OH. It is a

1385 lower limit as direct emissions could have left the domain during the simulation or have
 1386 undergone deposition. Thus we confirm that sulfate formed from atmospheric oxidation of
 1387 SO₂ is the dominant driver of the plume halogen chemistry on the regional scale. This
 1388 contrasts to the near-downwind plume where the directly emitted sulfate (formed from high-
 1389 temperature SO₃) is dominant and is essential for the rapid formation of BrO (see Roberts et
 1390 al., 2009, von Glasow, 2010).

1391 Figure 11 shows the spatial distribution of sulfate due to Ambrym emissions calculated as the
 1392 daily mean difference between the simulation S1_HighT and S0 for 12th January 2005. The
 1393 vertical profile of this daily averaged (across the domain) sulfate is also shown in Figure 12
 1394 for S1_HighT and S0 simulations. This Figure shows that the contribution of Ambrym to the
 1395 sulfate in the domain is mostly confined below 600 hPa. ~~The~~ Figure 11 indicates that it can
 1396 reach 2.5 ppbv in the plume at 875 hPa, the approximate altitude of the emissions injection in
 1397 the simulation. The contribution of Ambrym is also particularly high (hundreds of pptv) in an
 1398 extensive zone west of the volcano at 875 hPa. ~~In~~ the middle troposphere (500 hPa) and in
 1399 the Tropical Tropopause Layer (150 hPa), the influence of Ambrym is more localized. It is
 1400 co-localized with convective events as can be seen in the precipitation data of the TRMM
 1401 (Tropical Rainfall Measuring Mission) satellite (Huffman et al., 2007) and simulated by the
 1402 model (Figure 13). More precisely, the 500 hPa enhancement is co-localized with a band of
 1403 convective systems situated south east of New Caledonia the 12th and in the days prior. This is
 1404 further confirmed by the analysis of forward trajectories initialized from Ambrym on the
 1405 ~~10th~~ 10th and ~~the~~ 11th of January 2005 (Figure 14) calculated with the HYSPLIT transport and
 1406 dispersion model (Draxler and Rolph, 2003). The enhancement of sulfate at 150 hPa is co-
 1407 localized with a convective event that happened north of Vanuatu on the ~~11th~~ 11th as
 1408 suggested by the TRMM data (not shown) and could also ~~be resulting~~ result from transport
 1409 from a convective event that occurred to the south as shown in Figure 13. These localized

enhancements of sulfate in the middle and upper troposphere due to Ambrym can reach 700 pptv at 500 hPa and 250 pptv at 150 hPa. Overall, over the whole domain, above 600 hPa, the influence of Ambrym emissions is reduced: sulfate mixing ratios are increased by 30 pptv for example at 300hPa. This is explained by the fact that sulfate ~~is~~[aerosols are](#) strongly washed-out by precipitation in the model. In this model study, the aqueous-phase oxidation of SO₂ to sulfate was not taken into account. This process becomes self-limiting in strong volcanic plumes due to the titration of oxidants for example H₂O₂ (Schmidt et al., 2010) but may have a significant contribution to sulfate formation over the whole model domain~~thus, especially~~[because the region studied is particularly cloudy as shown by Figure 13. Thus this](#) will be considered in future work.

Mis en forme : Police :Non Gras

[Total aerosol optical depth \(AOD\) at 550 nm from MODIS/Aqua is also shown in Figure 5s of supplementary material for the 9-16 January 2005. Enhanced AOD are clearly seen southeast of Ambrym in the direction taken by the plume the 12th January 2005 as discussed earlier \(see Figure10\) as well as northwest of Ambrym in the direction of trades winds. The latter point is again consistent with OMI SO₂ images from GSFC \(Goddard Space Flight Center\) at \[http://so2.gsfc.nasa.gov/pix/daily/0105/vanuatu_0105z.html\]\(http://so2.gsfc.nasa.gov/pix/daily/0105/vanuatu_0105z.html\) showing that the plume was carried toward the northwest on the 14th and 15th January 2005. Figure 5s shows that enhanced AOD values varies between 0.12 and 0.34, which are approximately twice higher than the 3 years average \(Oct.2005-Oct.2008\) AOD from MODIS presented by Lefevre et al. \(2015\). This is consistent with the extreme passive degassing activity of Ambrym during January 2005. This confirms the strong influence of Ambrym on the budget of sulfate aerosol in the South West Pacific region and is qualitatively in agreement with our results.](#)

4.2.2 Bromine

Figure 15 shows the horizontal distribution of the total bromine content ($Br_y = HBr + 2Br_2 + BrCl + Br + BrO + HOBr + BrONO_2$) due to Ambrym emissions calculated as the daily mean difference between the simulation S1_HighT and S0 for 12th January 2005. The vertical profile of this daily averaged Br_y is shown in Figure 16 for S1_HighT and S0 simulations. The results presented here are for the larger grid whose resolution is 50 km ~~×~~ 50 km. The regional influence of Ambrym volcano emissions as a source of Br_y is clearly demonstrated. Ambrym is the main volcanic source of bromine in the domain, causing a regional plume of enhanced Br_y (maximum of 60 pptv) in the lower troposphere. Bagana volcano in Papua New Guinea was also active at this time (see section 2.3.3.1), and is responsible for a smaller enhancement in the S0 simulation around 875 hPa seen in Figure 16. In the middle troposphere (500 hPa) and in the Tropical Tropopause Layer (150 hPa), the influence of Ambrym is still visible but more localized, increasing locally the background Br_y by up to 3 pptv. The same convective events as those mentioned in the previous section are responsible for these Br_y enhancements. There is also evidence of transport to the stratosphere when analysing results at 80 hPa (a model level that is above the thermal tropopause in the simulation) with a few visible patches of Br_y of up to 0.5 pptv. Such transport of volcanic bromine to the upper troposphere and the stratosphere is of strong interest. Indeed, the stratospheric bromine burden is underestimated by global models that only take ~~only~~ into account long lived halons and methyl bromide. The missing source is believed to arise from bromine containing very short lived substance (VSLS) (i.e: bromocarbon source gases whose lifetime is less than 6 months, their degradation products as well as inorganic sources of bromine in the troposphere) transported from the boundary layer to the stratosphere. Their contribution to the stratospheric bromine loading ranges between 2-8 pptv (Carpenter et al., 2014). Here, we find that bromine emissions from Ambrym are responsible for a mean increase of 0.3 pptv of Br_y in the model domain at the altitude of the plume (875 hPa), and of

Mis en forme : Indice

Mis en forme : Indice

Mis en forme : Indice

Mis en forme : Indice

Mis en forme : Indice

Mis en forme : Indice

Mis en forme : Indice

0.1 pptv around 300 hPa in the upper troposphere (Figure 16). ~~Locally~~Local enhancements of 3 pptv are simulated in the upper troposphere due to convective transport and there is also evidence of transport to the stratosphere (up to 80 hPa) of Br_y from Ambrym as mentioned above. Figure 16 also presents the vertical profile of daily mean Br-speciation of volcanic Br_y . We have only considered the model grid boxes strongly influenced by volcanic bromine (for which the mean difference between S1_HighT and S0 was higher than 0.5 pptv in Figure 21). It is clear from this figure that the partitioning strongly varies with altitude. In the lower troposphere, as seen previously at the local scale in Section 3.2, HBr is readily depleted by its conversion into reactive bromine by the reaction of HOBr on sulfate aerosol, that produces Br_2 and/or BrCl . BrCl dominates which is surprising as it is readily photolysed, and was not found to be a major component of reactive bromine at the local plume-scale (section 3.2). This is most likely due to very rapid halogen cycling on sulfate aerosol, whose concentration increases as more volcanic SO_2 is oxidized in the downwind plume. HOBr also contributes to a significant fraction of Br_y at the regional scale at 875 hPa consistent with its role of reservoir of reactive bromine when the plume becomes diluted. The greater influence of photolysis reactions at higher altitudes is shown in the profiles by the declining HOBr and increasing Br with altitude that causes BrO also to increase. HOBr can also be washed out by precipitation. There is a back-conversion of reactive bromine species (Br and BrO) into HBr at higher altitude above 300 hPa. It is caused by reaction of volcanic Br with HO_2 . Note that the difference between Br_y from S1 and from S1_HighT (not shown) is small and can reach a maximum of 3 pptv in regions of Ambrym plume that reach up to 60 pptv Br_y at 875 hPa.

Mis en forme : Indice

Mis en forme : Indice

Mis en forme : Indice

Mis en forme : Indice

4.2.3 Ozone

Figure 17 shows the variation of ozone due to Ambrym emissions calculated as the daily mean difference in percent (of S0) between the simulation S1_HighT and S0 for 12th January 2005. The magnitude of ozone depletion in the simulation S1_HighT is correlated with the

change ~~of~~[in](#) sulfate and ~~of~~[in](#) bromine due to Ambrym emissions (Figures 11 and 15).— At 875 hPa, it is maximal (40 %) in the concentrated plume and significant (> 10 %)- in an extensive zone west of the volcano strongly influenced by Ambrym emissions (Figures 11 and 15). Note that during the day, the depletion can be total in the plume (not shown) as presented at plume scale (Figure 8). Transport of an ozone depleted air mass by convection can also be seen at 500 hPa. At higher altitudes, the influence of Ambrym on ozone mixing ratios is smaller, less than 2%. When the whole domain is considered, Ambrym emissions are responsible for an ozone depletion of 72 Gg in the S1_HighT simulation, it represents 0.2% of the ozone content in the domain (32 Tg of ozone). In the S1 simulation, depletion of ozone due to Ambrym totals 69 Gg of ozone. It is consistent with the fact that high temperature chemistry [initialization](#) is only important in approximately the first 150 ~~kilometres~~[kilometers](#) from the source in our simulation as shown in section 3.2.

1496 **4.3 Impact of Ambrym emissions on the oxidizing power of the troposphere**

1497 The oxidizing capacity of the troposphere determines the atmospheric fate of many atmospheric pollutants including greenhouse gases such as methane, thus is an important control on tropospheric composition and climate. Volcanic emissions are expected to impact the oxidizing power of the atmosphere in several ways. First, the large amounts of SO₂ emitted by volcanoes react with OH, drastically reducing its concentration. Furthermore, the conversion of emitted halogen halides to more reactive halogen species in volcanic plumes results in chemical cycles that deplete ozone and HO₂ (and therefore OH), as well as NO_x that can in turn also affect ozone and OH. In addition, these reactive halogen cycles produce chlorine radicals that can also oxidize methane and non-methane hydrocarbons. Here, to illustrate the impact of Ambrym during the extreme degassing event of January 2005 on the oxidizing capacity of the atmosphere, we calculate change to the lifetime of a key atmospheric greenhouse ~~gas~~[gas](#): methane. In particular, we investigate the relative contribution of the

1509 different components of the volcanic emissions to the overall perturbation of methane lifetime
1510 due to Ambrym degassing.

1511 Methane is a key greenhouse gas with both natural and anthropogenic sources, whose main
1512 loss pathway from the atmosphere is by gas-phase reaction with OH. Methane lifetime due to
1513 a process (e.g., reaction with OH) is commonly defined as the total methane atmospheric
1514 burden (Tg) at steady state (i.e. with unchanged burden) divided by total methane losses
1515 through this process (Tg/yr) (IPCC, 2001). -We have applied this definition here. However, it
1516 is important to highlight that to calculate a proper methane lifetime we would have to perform
1517 a simulation of about 10 years with a global model. Instead, we have calculated the
1518 instantaneous perturbation of CH₄ lifetime over the model domain (averaged over a day),
1519 which reflects the instantaneous perturbation of the methane sink on a regional scale. The
1520 results in terms of lifetime change cannot be extrapolated to the global scale and depend also
1521 strongly on the area of the model domain. Our aim here is to assess the relative contribution
1522 of volcanic sulfur emissions and reactive halogen plume chemistry on the overall perturbation
1523 of CH₄ lifetime.

1524 We calculate that the methane lifetime due to reaction of methane with OH, $\tau_{\text{CH}_4+\text{OH}}$, is
1525 about 4.65 years in our simulation when the volcanic emission from Ambrym is not included.
1526 A value of 9.7 +/- 1.5 yr is derived from most recent studies based on global modeling (Naik
1527 et al., 2012). The shorter methane lifetime calculated here reflects the condition in the tropics
1528 for January where the OH concentration is particularly high. We find that $\tau_{\text{CH}_4+\text{OH}}$ increases
1529 by 0.97 % due to volcanic emissions in the simulation S1_HighT compared to the simulation
1530 S0. For the simulation with volcanic SO₂ emissions alone (S1_nohal), we calculate that the
1531 methane lifetime $\tau_{\text{CH}_4+\text{OH}}$ increase is only about 0.37%. Therefore ~~we infer that about 62%~~

1532 ~~of the increase of τ_{CH_4} in methane lifetime, with respect to OH, due to volcanic emissions is~~
1533 ~~due to~~ enhanced by a factor of 2.6 when reactive halogen chemistry ~~cycles that deplete HO_x~~
1534 ~~and ozone. is considered.~~

Mis en forme : Police :12 pt, Non
Exposant/ Indice

Mis en forme : Police :12 pt

Mis en forme : Couleur de police :
Bleu, Anglais (Royaume-Uni), Non

Mis en forme : Non Barré

1535 A second consideration is that the volcano plume chlorine can itself react with methane,
1536 decreasing its lifetime. The methane lifetime due to reaction with Cl, $\tau_{\text{CH}_4+\text{Cl}}$ is 246 years in
1537 our simulation without volcanic emission from Ambrym (S0). This compares well to the
1538 methane lifetime of about 200 yr derived by Allan et al. (2007). When Ambrym emissions are
1539 included, $\tau_{\text{CH}_4+\text{Cl}}$ decreases by 17 % to 204 years due to reaction with reactive chlorine
1540 produced in Ambrym plume. Nevertheless, this reduction in methane lifetime due to Cl
1541 radicals only partially counters the increase in methane lifetime caused by the decrease of OH
1542 (through both volcanic plume halogen cycles and SO₂). The net volcanic impact is an overall
1543 0.57 % increase in methane lifetime. Thus, the effect of chlorine radicals on the methane
1544 lifetime counteracts 41% of the effect due to the OH decrease. Note that very recent
1545 measurements of reactive chlorine (OCIO) in Mt Etna volcanic plume (General et al., 2014;
1546 Gliß et al., 2015) could help to better quantify the impact of chlorine radicals on the methane
1547 lifetime.

1548 4.4 Impact of Ambrym emissions on SO₂ lifetime

1549 As already discussed in the Introduction, SO₂ undergoes atmospheric oxidation into sulfate
1550 aerosols that exert climatic impacts from both direct radiative and indirect cloud albedo
1551 effects (Schmidt et al., 2012). Sinks of SO₂ are dry and wet deposition, gas phase oxidation
1552 and aqueous phase oxidation. The estimated lifetime of SO₂ in the troposphere by global
1553 models ranges between 0.6-2.6 days (e.g., Rotstajn and Lohmann, 2002 and references
1554 therein), with a lifetime with respect to gas-phase oxidation by OH of around 2 weeks (e.g.,

1555 Rotstayn and Lohmann, 2002; Von Glasow 2009). However, model studies indicate a
1556 lengthened lifetime for volcanic SO₂ (e.g., Chin and Jacob, 1996; Graf et al., 1997; Stevenson
1557 et al., 2003; Schmidt et al., 2010). For example, a lifetime of 24-34 days was calculated for
1558 the Laki 1783-4 eruption using a global model (Schmidt et al., 2010). This is due to volcanic
1559 plume injection into the free troposphere (where removal rates are much lower than in the
1560 boundary layer) and suppression of oxidants (OH, H₂O₂, noting limited role of ozone under
1561 acid conditions) by the SO₂ chemistry. Our regional 3D model study includes a less detailed
1562 SO₂-sulfate chemistry scheme (gas-phase oxidation only) but includes detailed plume reactive
1563 halogen chemistry. Here, we have calculated the impact of volcanic halogen chemistry on the
1564 lifetime of SO₂ due to gas phase oxidation by OH. More precisely, we calculate the lifetime of
1565 SO₂ in the whole domain and of SO₂ in the plume from Ambrym (defined in our study as
1566 model grids where SO₂ > 5 ppbv). For the simulation S1_nohal (that includes only SO₂
1567 emissions) and for the whole domain of the simulation, we find ~~an SO₂ lifetime of~~ an SO₂ lifetime of 8.8
1568 days consistent with previous work given that the simulation is for the tropics. For this
1569 S1_nohal simulation and considering only the plume of Ambrym, the lifetime of SO₂
1570 increases (11 days). This is consistent with the known self-limitation of SO₂ oxidation in
1571 volcanic plumes as OH becomes depleted in the plume by the reaction with SO₂ itself. For the
1572 simulation including volcanic halogens with high-temperature initialization, S1_HighT, the
1573 SO₂ lifetime for the whole domain is 8 days and for the plume 5.5 days. This result of shorter
1574 SO₂ lifetime in the plume than in the whole domain is initially surprising because of the self-
1575 limitation of SO₂ oxidation as explained above. The shorter SO₂ lifetimes for
1576 S1_HighT ~~compared~~ compared to S1_nohal are also again surprising because the
1577 halogen chemistry acts to further deplete OH in the plume. These results are explained by the
1578 OH emissions in S1_HighT (high-temperature initialization) that provides an additional rapid
1579 near-source sink for SO₂, thereby contributing to the effective volcanic sulfate emission. This

1580 is confirmed by the simulation, S1_nohal2 (that includes SO₂ emissions and OH emissions
1581 from HSC chemistry but no halogens), in which the SO₂ lifetimes are 7.5 days for whole
1582 domain and 5.6 days for the plume. This impact of high-temperature OH source on volcanic
1583 SO₂ occurs very close to source (after which OH becomes depleted), leading to an unexpected
1584 shortening of the calculated SO₂ lifetime, that complicates the lifetime calculation. A similar
1585 effect was not seen for methane because it is not co-emitted from the volcano and OH is
1586 preferentially titrated by SO₂ (and HCl).

1587 Because of the complication of the lifetime calculation in S1_HighT, it is better to compare
1588 the simulations with (S1) and without (S1_nohal) halogen emissions, excluding high-
1589 temperature chemistry. We have shown before that simulations with and without high
1590 temperature chemistry give very similar results in terms of Br_y and ozone at the regional scale
1591 (see sections 4.2.2 and 4.2.3). In the simulation S1, the SO₂ lifetime is 15 days in the plume
1592 and 9.4 days for the whole domain. This results is consistent with what it is expected as the
1593 lifetime of SO₂ is lengthened in the plume compared to the S1_nohal (SO₂ emission only)
1594 simulation (11 days). We conclude that [including](#) volcanic halogen chemistry increases the
1595 lifetime of SO₂ in the plume by 36 % through its impact on OH. Similarly, SO₂ lifetime is also
1596 increased by halogen chemistry for the whole domain, but by a lesser extent (9.4 days
1597 compared to 8.8 days in S1_nohal).

Mis en forme : Indice

1598 5. Conclusions

1599 The CCATT-BRAMS meso-scale model was used and further developed to study the impact
1600 of Ambrym volcano emissions, Vanuatu (Southwest Pacific), on the chemical composition of
1601 the atmosphere at the local and regional scales. We focus on an episode of extreme passive
1602 degassing of Ambrym that lasted several months in early 2005, and for which SO₂ and BrO
1603 columns [from](#) airborne DOAS measurements in the plume have been reported. Model
1604 development includes the incorporation of reactive halogen chemistry and a volcano emission

1605 source specific to Ambrym. Using the nesting grid capability of CCATT-BRAMS, we
1606 simulate the Ambrym plume at high resolution ($500\text{ m} \times 500\text{ m}$). This allows us to make a
1607 ~~direct (unbiased)~~ “point by point” comparison with DOAS SO_2 and BrO data, and hence test
1608 our understanding of volcanic plume chemistry at the plume level. We find that the model
1609 reproduces reasonably well the spatial distribution of SO_2 in the near downwind plume (i.e.
1610 the direction and dilution of the plume). The model captures the salient features of volcanic
1611 chemistry as reported in previous work such as HO_x and ozone depletion in the core of the
1612 plume. With the simulation initialized with high temperature chemistry at the vent (that
1613 produces: Br, Cl, HO_x and NO_x radical species), the pattern of BrO/ SO_2 trend with distance
1614 downwind and across the plume simulated by the model is in good agreement with the DOAS
1615 observations. However, the model underestimates by 60% the magnitude of ~~the~~
1616 ~~maximal observed~~ BrO ~~enhancement~~ columns in the near downwind plume ~~is underestimated~~
1617 ~~by the model by a factor 3 at 15 km.~~ The analysis of the model results shows that BrO
1618 formation is ozone limited in the near-downwind (concentrated) plume due to the
1619 combination of a low background ozone (15 ppbv, of which 100% is depleted in the plume)
1620 and the high emissions flux from Ambrym.
1621 Further downwind in the plume at 40 km, we find a much better agreement between observed
1622 and modelled Bro columns (mean bias of 14%). This study confirms the importance of the
1623 high temperature chemistry at the vent to reproduce BrO/ SO_2 variation in the near downwind
1624 plume. It also demonstrates that the (non-sulfur) radicals produced by the high temperature
1625 chemistry are mostly important for the initial rise of BrO/ SO_2 at Ambrym. Further downwind
1626 from the vents (after 150 km approximately for our case), simulations with and without the
1627 high-temperature initialization exhibit rather similar chemistry. Nevertheless, the primary
1628 aerosol emission, that is crucial to enable the heterogeneous chemistry producing reactive
1629 bromine in the near downwind plume, originates from the high-temperature plume chemistry

1630 at the vent. It was kept constant in these simulations (at 1% of total sulfur) and hence its
1631 impact is not taken into account when comparing simulations with and without high
1632 temperature chemistry.

1633 ~~Impacts of Ambrym in Southwest Pacific region were also evaluated~~[Our 3D regional model](#)
1634 [approach allows us to make the link between near downwind plume observations and regional](#)
1635 [scale observations given by satellite data. Here, we show that the model when initialized with](#)
1636 [the Ambrym SO₂ source strength estimate derived from the DOAS observations by Bani et al.](#)
1637 [\(2009\) and \(2012\) simulates SO₂ columns at the regional scale that agree within 25 % with](#)
1638 [the SO₂ columns detected by OMI. Impacts of Ambrym in Southwest Pacific region were also](#)
1639 [analyzed](#) across the larger model grid domain. In the lower troposphere, at altitudes close to
1640 the injection height (875 hPa), Ambrym causes a substantial increase in sulfate (from 0.1
1641 ppbv to 2.5 ppbv) and in bromine mixing ratios (from 0.1 pptv to 60 pptv). Transport of
1642 bromine species (as well as sulfate) to the upper troposphere due to convection is also
1643 predicted by the model, with convective regions confirmed by the precipitation data from the
1644 TRMM satellite as well as by trajectories from the HYSPLIT transport and dispersion model.
1645 There is also evidence in the simulations of a subsequent transport of bromine to the
1646 stratosphere from Ambrym. [Thus, the halogen activation in tropospheric volcanic plumes](#)
1647 [could be one aspect of the potential impact of volcanic halogen on stratospheric ozone.](#) In
1648 future work, longer duration simulations should be performed to fully quantify the impact of
1649 Ambrym on chemical composition of the troposphere at the regional scale. In particular, flux
1650 of bromine to upper troposphere and to the stratosphere from this extreme continuous
1651 degassing event, as well as during the typical continuous emission from Ambrym should be
1652 calculated. This will provide insight to the importance of Ambrym volcano plume to the
1653 budget and chemistry of bromine in these regions. Ozone depletion (between 5 % to 40 %) is
1654 ongoing albeit slower in the extensive region few thousands of kilometres from the volcano

1655 influenced by the dispersed plume. We find a tropospheric ozone depletion of 72 Gg, (i.e.,
1656 0.2% for a domain containing 32 Tg of ozone) in the model domain.

1657 This influence of the plume chemistry on tropospheric oxidants (depletion of HO_x and ozone
1658 by reactive halogen chemistry and depletion of OH by oxidation of SO₂) in turn affects other
1659 atmospheric species in the model. We show that methane lifetime (with respect to its reaction
1660 with OH and with Cl) in the model is increased when volcanic emissions are taken into
1661 account, confirming the potential for volcanic emissions to influence the oxidizing power of
1662 the atmosphere. Furthermore, ~~we find that reactive halogen chemistry is responsible for more~~
1663 ~~than half of the perturbation (62%) of increase in~~ methane lifetime, with respect to oxidation
1664 by OH, with depletion due to volcanic emissions is enhanced by a factor of OH by SO₂ 2.6
1665 when reactive halogen chemistry responsible for the remainder is considered. Cl radicals
1666 produced in the plume counteract some of the effect (41%) of the methane lifetime
1667 lengthening due to OH depletion. This work thereby particularly highlights the impact of
1668 reactive volcanic halogen chemistry on the oxidizing capacity of the atmosphere. Here, it is
1669 found to be more important than the impact of OH depletion by volcanic SO₂. However, the
1670 reactive halogen mediated HO_x depletion and Cl radical formation exert opposing impacts on
1671 the methane lifetime. Furthermore, we calculate an increase of 36% in the SO₂ lifetime with
1672 respect to oxidation by OH ~~due to when~~ reactive halogen chemistry in the plume ~~that depletes~~
1673 ~~HO_x and ozone~~ are included in the simulations. Thus reactive halogen chemistry exerts a
1674 significant influence on the volcanic SO₂ lifetime hence also on the production of sulfate.

1675 This needs to be taken into account in studies evaluating the impact of volcanoes on radiative
1676 forcing. ~~Especially, especially~~ if the injection height is high in altitude, (where the sink of SO₂
1677 by OH can be the dominant oxidation pathway and thus exert a major control on SO₂ lifetime
1678 and sulfate formation ~~(Schmidt et al., 2010).~~ Schmidt et al., 2010). Wash-out processes

Mis en forme : Anglais (États Unis)

Mis en forme : Anglais (États Unis)

Mis en forme : Anglais (États Unis)

Mis en forme : Anglais (États Unis)

Mis en forme : Anglais (États Unis)

Mis en forme : Anglais (États Unis)

1679 [were included in the model but aqueous phase of oxidation of SO₂ was not. In future this](#)
1680 [should also be included in the model, given the cloudiness of the Vanuatu region.](#)

1681 Uncertainties in the modelled plume chemistry include aspects of the volcanic emissions, and
1682 also the rate of heterogeneous reaction of HOBr on the volcanic aerosol, which is a key driver
1683 of the reactive halogen cycling hence the plume regional impacts. This depends on the aerosol
1684 surface area and underlying chemical kinetics (for which a re-evaluation for acidic plume
1685 conditions was made by Roberts et al., 2014b). Ongoing work is aimed at improving the
1686 aerosol and HOBr reactive uptake parameterization in the model. Transects across the plume
1687 at various distances from the vents, as performed by Bani et al. (2009), appear very useful
1688 altogether with a model to test our understanding of the dynamics of volcanic plume
1689 chemistry. Nevertheless, this study emphasizes the need to measure more chemical species to
1690 constrain knowledge of the volcanic plume chemistry as also highlighted in

1691 ~~Bobowski~~[Bobrowski](#) et al. (2015). In particular, the coupling between BrO_x (= Br + BrO)
1692 and NO_x appears rather uncertain (Roberts et al., 2014a). Measurements of BrO and SO₂ are

1693 not sufficient to fully constrain the plume chemistry; background ozone as well as in plume
1694 ozone, HO_x, NO_x, as well as other bromine compounds than BrO and size-resolved aerosol

1695 characterisation are needed along with a better characterisation of the plume injection height
1696 and of the plume depth (width in general being constrained by satellite and DOAS transects).

1697 To be most insightful, studies should combine the systematic downwind plume investigation
1698 with (simultaneous) detailed crater-rim measurements to constrain the volcanic gas and
1699 aerosol emission. Recent advances in satellite detection of reactive halogen species in
1700 tropospheric volcanic plumes (Hörmann et al., 2013) may also be used in future regional and
1701 global model studies of volcanic activity impacts.

1702
1703

Mis en forme : Indice

Mis en forme : Indice

Mis en forme : Indice

Mis en forme : Indice

1704
1705
1706
1707
1708
1709
1710
1711
1712
1713
1714
1715
1716
1717
1718
1719
1720
1721
1722
1723
1724
1725
1726
1727

Acknowledgements

This work was supported by the LABEX VOLTAIRE (VOLatils- Terre Atmosphère Interactions - Ressources et Environnement) ANR-10-LABX-100-01 (2011-20). It also benefited from the financial support of the program LEFE of the Institut National des Sciences de l'Univers of CNRS (Centre National de la Recherche Scientifique) provided to the HEVA project.

The authors benefitted from the use of the cluster at the Centre de Calcul Scientifique en région Centre. We gratefully acknowledge Saulo Freitas (NOAA/ESRL/CPTEC) for his help with the CCATT-BRAMS model and Laurent Catherine (OSUC) for technical help with the cluster at Centre de Calcul Scientifique en région Centre. We thank P. Bani (IRD) and C. Oppenheimer (University of Cambridge) for providing their DOAS data, Virginie Marécal (CNRM/Météo-France) for initiating the project and Bruno Scaillet (ISTO) for providing some earlier HCl/SO₂ and HBr/SO₂ ratios.

We are grateful to the NOAA Air Resources Laboratory for the provision of the HYSPLIT Transport and dispersion model (<http://www.arl.noaa.gov/ready/hysplit4.html>).

Mis en forme : Police :Calibri, 11 pt

1728
1729
1730
1731
1732
1733
1734
1735
1736
1737
1738
1739
1740
1741
1742
1743
1744
1745
1746
1747
1748
1749

References

Aiuppa, A., C. Federico, A. Franco, G. Giudice, S. Gurrieri, S. Inguaggiato, S. Liuzzo, M. A. J. S. McGonigle, A. J. S., and Valenza, M.: Emission of bromine and iodine from Mount Etna volcano, *Geochemistry, Geophysics, Geosystems* *Geochem. Geophys. Geosyst.*, **6**, 8, Q08008, doi:10.1029/2005GC000965, 2005.

Allan, W., H. Struthers, and D. C. Lowe, Methane carbon isotope effects caused by atomic chlorine in the marine boundary layer: Global model results compared with Southern Hemisphere measurements, *J. Geophys. Res.*, **112**, D04306, doi:10.1029/2006JD007369, 2007.

Allard, P., Aiuppa, A., Bani, P., Metrich, N., Bertagnini, A., Gauthier, P. J., Parelli, F., Sawyer, G. M., Shinohara, H., Bagnator, E., Mariet, C., Garebiti, E., and Pelletier, B.: Ambrym basaltic volcano (Vanuatu Arc): volatile fluxes, magma degassing rate and chamber

Mis en forme : auteur

Mis en forme : auteur

Mis en forme : Espace Avant : 6 pt, Après : 0 pt, Ne pas ajuster l'espace entre le texte latin et asiatique, Ne pas ajuster l'espace entre le texte et les nombres asiatiques

Mis en forme : Citation HTML

Mis en forme : auteur

Mis en forme : auteur

Mis en forme : auteur

Mis en forme : Citation HTML

Mis en forme : auteur

Mis en forme : auteur

Mis en forme : auteur

Mis en forme : auteur

Mis en forme : Citation HTML

Mis en forme : auteur

Mis en forme : auteur

Mis en forme : Citation HTML

Mis en forme : articletitle

Mis en forme : Citation HTML

Mis en forme : Citation HTML

Mis en forme : vol

Mis en forme : Citation HTML

Mis en forme : Citation HTML

Mis en forme : Espace Avant : 6 pt, Après : 0 pt

Mis en forme : Français (France)

Mis en forme : Français (France)

Mis en forme : Espace Avant : 6 pt, Après : 0 pt, Ne pas ajuster l'espace entre le texte latin et asiatique, Ne pas ajuster l'espace entre le texte et les nombres asiatiques

1750 depth. In, in: AGU Fall Meeting Abstracts (, Vol. 1, p. 04), San Francisco, United States of
1751 America, December, 2009.

1752 Allard, P., Aiuppa, A., Bani, P., ~~Metric~~Métrich, N., Bertagnini, A., Gauthier, P., J.,
1753 Shinohara, H., Sawyer, G., ~~M., Parelli.,~~ Parello, F., ~~Bagnator~~Bagnato, E., and Pelletier, B. and
1754 ~~Garebiti E.:~~ Prodigious emission rates and magma degassing budget of major, trace and
1755 radioactive volatile species from Ambrym basaltic volcano, Vanuatu ~~Arc, submitted to~~
1756 ~~Journal of Volcanology and Geothermal Research,~~ island Arc, J. Volcanol. and Geoth. R.,
1757 ~~, doi:10.1016/j.jvolgeores.2015.10.004, in press~~ 2015.

1758 Allibone, R., Cronin, S.J., Douglas, C.T., Oppenheimer, C., Neall, V.E., Stewart, R.B.: Dental
1759 fluorosis linked to degassing on Ambrym volcano, Vanuatu: a novel exposure, pathway.
1760 Environmental Geochemistry and Health, doi:10.1007/s10653-010-9338-2, 2010.

1761 Andres, R. J., and Kasgnoc A. D.: A time-averaged inventory of subaerial volcanic sulfur
1762 emissions, Journal of Geophysical Research: Atmospheres (1984–2012), 103, no. D19 25251-
1763 25261, 1998.

1764 Arteta, J., Marécal, V., and Riviere, E. D.: Regional modelling of tracer transport by tropical
1765 convection–Part 1: Sensitivity to convection parameterization. Atmospheric Chemistry and
1766 Physics, 9, 18, 7081-7100, 2009a.

1767 Arteta, J., Marécal, V., and Riviere, E. D. Regional modelling of tracer transport by tropical
1768 convection–Part 2: Sensitivity to model resolutions. Atmospheric Chemistry and Physics,
1769 9(18), 7101-7114, 2009b.

1770 Atkinson, R., Baulch, D. L., Cox, R. A., Crowley, J. N., Hampson, R. F., Hynes, M. E.
1771 Jenkin, M. J. Rossi, and Troe J.: Evaluated kinetic and photochemical data for atmospheric

Mis en forme : Espace Avant : 6 pt,
Après : 0 pt

1772 chemistry: Volume III–gas phase reactions of inorganic halogens. Atmospheric Chemistry
1773 and Physics, 7, 4, 981-1191, 2007.

1774 Bani, P., Oppenheimer C., Tsanev V. I., Carn S. A., Cronin S. J., Crimp R., Calkins J. A.,
1775 Charley D., Lardy M. and Roberts T. R.: Surge in sulphur and halogen degassing from
1776 Ambrym volcano, Vanuatu, Bulletin of Volcanology 71, 10, 1159-1168, 2009.

1777 Bani, P., Oppenheimer C., Allard P., Shinohara H., Tsanev V., Carn S., Lardy M., Garaebiti
1778 E.: First estimate of volcanic SO₂ budget for Vanuatu island arc, Journal of Volcanology and
1779 Geothermal Research, 211, 36-46, 2012.

1780 Barrie, L. A., Bottenheim, J. W., Schnell, R. C., Crutzen, P. J., and Rasmussen, R. A.:
1781 Ozone ~~destruction~~Destruction and ~~photochemical reactions~~Photochemical Reactions at ~~polar~~
1782 ~~sunrise~~Polar Sunrise in the ~~lower~~Lower Arctic ~~atmosphere~~Atmosphere, Nature 334, 138–
1783 141, doi:10.1038/334138a0, 1988.

Mis en forme : Espace Avant : 6 pt,
Après : 0 pt, Ne pas ajuster l'espace
entre le texte latin et asiatique, Ne pas
ajuster l'espace entre le texte et les
nombres asiatiques

1784
1785 Bhartia, P. K., and ~~C. W.~~ Wellemeyer (2002), ~~C. W.~~ OMI TOMS-V8 Total O3 Algorithm,
1786 Algorithm Theoretical Baseline Document: OMI Ozone Products, edited by ~~P. K.~~ Bhartia,
1787 ~~vol~~P. K., Vol. II, ATBD-OMI-02, -version 2.0, available at: [http://eosps0.gsfc.nasa.gov/sites](http://eosps0.gsfc.nasa.gov/sites/default/files/atbd/ATBDOMI-ATBD-OMI-02.pdf)
1788 [/default/files/atbd/ATBDOMI-ATBD-OMI-02.pdf](http://eosps0.gsfc.nasa.gov/sites/default/files/atbd/ATBDOMI-ATBD-OMI-02.pdf) (last access: November 2015).

Mis en forme : Espace Avant : 6 pt,
Après : 0 pt, Ne pas ajuster l'espace
entre le texte latin et asiatique, Ne pas
ajuster l'espace entre le texte et les
nombres asiatiques

Mis en forme : Français (France)

Code de champ modifié

1789 Bela, M. M., Longo K. M., Freitas S. R., Moreira D. S., Beck V., Wofsy S. C., Gerbig C.,
1790 Wiedemann K., Andreae M. O. and Artaxo P.: Ozone production and transport over the
1791 Amazon Basin during the dry-to-wet and wet-to-dry transition seasons, Atmospheric
1792 Chemistry and Physics, 15, 757-782, 2015.

Mis en forme : Espace Avant : 6 pt,
Après : 0 pt

1793 Bobrowski, N., G. Hönninger, B. Galle, and U. Platt: Detection of bromine monoxide in a
1794 volcanic plume, Nature, 423, 6937, 273-276, 2003.

1795 Bobrowski, N., and U. Platt: SO₂/BrO ratios studied in five volcanic plumes, Journal of
 1796 Volcanology and Geothermal Research 166, 3, 147-160, 2007.

1797 Bobrowski, N., ~~Von~~R. von Glasow ~~R., A.~~ Aiuppa ~~A., S.~~ Inguaggiato ~~S., I.~~ Louban ~~I., O.~~
 1798 W. Ibrahim ~~O. W.,~~ and U. Platt ~~U.~~: Reactive halogen chemistry in volcanic plumes, ~~Journal~~
 1799 ~~of Geophysical Research: Atmospheres (1984-2012)~~J. Geophys. Res., 112, ~~D6~~D06311,
 1800 doi:10.1029/2006JD007206, 2007.

1801 Bobrowski, N., R. Glasow, G. B. Giuffrida, D. Tedesco, A. Aiuppa, M. Yalire, S. Arellano,
 1802 M. Johansson, and B. Galle.: Gas emission strength and evolution of the molar ratio of
 1803 BrO/SO₂ in the plume of Nyiragongo in comparison to Etna: Journal of Geophysical
 1804 Research: Atmospheres 120, 1, 277-291, 2015.

1805 Boichu, M., Oppenheimer C., Roberts T. J., Tsanev V., and Kyle P. R.: On bromine, nitrogen
 1806 oxides and ozone depletion in the tropospheric plume of Erebus volcano (Antarctica),
 1807 Atmospheric Environment, 45, 23, 3856-3866, 2011.

1808 Carn, S.A., L. Clarisse and A.J. Prata, Multi-decadal satellite measurements of global
 1809 volcanic degassing, J. Volcanol. Geotherm. Res.,
 1810 http://dx.doi.org/10.1016/j.jvolgeores.2016.01.002, 2016.

1811 Carpenter L. J. and S. Reimann (Lead Authors), J.B. Burkholder, C. Clerbaux, B.D. Hall, R.
 1812 Hossaini, J.C. Laube, and S.A. Yvon-Lewis, Ozone-Depleting Substances (ODSs) and Other
 1813 Gases of Interest to the Montreal Protocol, Chapter 1 in Scientific Assessment of Ozone
 1814 Depletion: 2014, Global Ozone Research and Monitoring Project – Report No. 55, World
 1815 Meteorological Organization, Geneva, Switzerland, 2014.

Mis en forme : Espace Avant : 6 pt,
Après : 0 pt

1816 Carslaw, K. S., L. A. Lee, C. L. Reddington, K. J. Pringle, A. Rap, P. M. Forster, G. W.
1817 Mann, Spracklen D. V., Woodhouse M. T., Regayre L. A. and Pierce J. R.: Large contribution
1818 of natural aerosols to uncertainty in indirect forcing, Nature 503, 7474, 67-71, 2013.

1819 Chin, M., and Jacob, D. J.: Anthropogenic and natural contributions to tropospheric sulfate: A
1820 global model analysis. Journal of Geophysical Research: Atmospheres (1984–2012), 101,
1821 D13, 18691-18699, 1996.

1822 Delmelle, P.: Environmental impacts of tropospheric volcanic gas plumes. Special
1823 Publication – Geological Society of London, 213, 381-400, 2003.

1824 Diehl, T., Heil, A., Chin, M., Pan, X., Streets, D., Schultz, M., and Kinne, S.: Anthropogenic,
1825 biomass burning, and volcanic emissions of black carbon, organic carbon, and SO2 from 1980
1826 to 2010 for hindcast model experiments, Atmos. Chem. Phys. Discuss., 12, 24895-24954,
1827 doi:10.5194/acpd-12-24895-2012, 2012.

1828 Draxler, R. R. and Rolph, G. D.: HYSPLIT (HYbrid Single-Particle Lagrangian Integrated
1829 Trajectory) Model access via NOAA ARL READY Website (available at:
1830 <http://ready.arl.noaa.gov/HYSPLIT.php>), (last access: November 2015).

1831 Fan, S.-M. and Jacob, D. J.: Surface ozone depletion in Arctic spring sustained by bromine
1832 reactions on aerosols, Nature, 359, 522–524, 1992.

1833 Freitas, S. R., Longo, K. M., Silva Dias, M. A. F., Chatfield, R., Silva Dias, P., Artaxo, P.,
1834 Andreae, M. O., Grell, G., Rodrigues, L. F., Fazenda, A., and Panetta, J.: The Coupled
1835 Aerosol and Tracer Transport model to the Brazilian developments on the Regional
1836 Atmospheric Modeling System (CATT-BRAMS) – Part 1: Model description and evaluation,
1837 Atmos. Chem. Phys., 9, 2843-2861, doi:10.5194/acp-9-2843-2009, 2009.

Mis en forme : Couleur de police : Noir

Mis en forme : Couleur de police : Noir

Mis en forme : Couleur de police : Noir

Mis en forme : Français (France)

Code de champ modifié

Mis en forme : Couleur de police : Noir

Mis en forme : Couleur de police : Noir

1838 Freitas, S. R., Longo K. M., Alonso M. F., Pirre M., Marecal V., Grell G., Stockler R., Mello
1839 R. F., and Sánchez Gácita M.: PREP-CHEM-SRC-1.0: a preprocessor of trace gas and
1840 aerosol emission fields for regional and global atmospheric chemistry models, Geoscientific
1841 Model Development, 4, 2, 419-433, 2011.

1842 ~~Gerlach, T. M.: Volcanic sources of tropospheric ozone-depleting trace gases, Geochemistry,~~
1843 ~~Geophysics, Geosystems 5, 9, 2004.~~

1844 General, S., Bobrowski, N., Pöhler D., Weber, K., Fischer, C., and Platt, U.: Airborne I-
1845 DOAS measurements at Mt. Etna: BrO and OCIO evolution in the plume, ~~Journal of~~
1846 ~~Volcanology and Geothermal Research, 2014~~J. Volcanol. Geoth. Res., 300, 175–186,
1847 doi:10.1016/j.jvolgeores.2014.05.012, 2015.

1848 ~~Gliß, J.,~~Gerlach, T. M.: Volcanic sources of tropospheric ozone-depleting trace gases,
1849 Geochem. Geophys. Geosyst., 5, Q09007, doi:10.1029/2004GC000747, 2004
1850 Gliß, J., Bobrowski, N., Vogel, L., Pöhler, D., and Platt, U.: OCIO and BrO observations in
1851 the volcanic plume of Mt. Etna – implications on the chemistry of chlorine and bromine
1852 species in volcanic plumes, Atmos. Chem. Phys., 15, 5659-5681, doi:10.5194/acp-15-5659-
1853 2015, 2015.

1854 Graf, H. F., Feichter J., and Langmann B.: Volcanic sulfur emissions: Estimates of source
1855 strength and its contribution to the global sulfate distribution, Journal of Geophysical
1856 Research: Atmospheres (1984–2012), 102, D9, 10727-10738, 1997.

1857 Grellier, L., Marécal, V., Josse, B., Hamer, P. D., Roberts, T. J., Aiuppa, A., and Pirre, M.:
1858 Towards a representation of halogen chemistry within volcanic plumes in a chemistry
1859 transport model. Geoscientific Model Development Discussions, 7, 2, 2581-2650, 2014.

Mis en forme : Espace Avant : 6 pt,
Après : 0 pt

Mis en forme : Police : Times New
Roman

1860 Guenther, A., Karl, T., Harley, P., Wiedinmyer, C., Palmer, P. I., and Geron, C.: Estimates of
 1861 global terrestrial isoprene emissions using MEGAN (Model of Emissions of Gases and
 1862 Aerosols from Nature), *Atmos. Chem. Phys.*, 6, 3181-3210, doi:10.5194/acp-6-3181-2006,
 1863 2006.

1864 Halmer, M. M., Schmincke H-U., and Graf H-F.: The annual volcanic gas input into the
 1865 atmosphere, in particular into the stratosphere: a global data set for the past 100 years, *Journal*
 1866 *of Volcanology and Geothermal Research*, 115, 3, 511-528, 2002.

1867 Hebestreit, K.; Stutz, J.; Rosen, D.; Matveiv, V.; Peleg, M.; Luria M.; Platt, U.: DOAS
 1868 measurements of tropospheric bromine oxide in mid-latitudes, *Science*, 283, 55–57, 1999.

1869 Hörmann, C., Sihler H., Bobrowski N., Beirle S., Penning de Vries M., Platt U., and Wagner
 1870 T.: Systematic investigation of bromine monoxide in volcanic plumes from space by using the
 1871 GOME-2 instrument., *Atmos. Chem. Phys*, 13, 4749-4781, 2013.

1872 Huffman, G.J., R.F. Adler, D.T. Bolvin, G. Gu, E.J. Nelkin, K.P. Bowman, Y. Hong, E.F.
 1873 Stocker and Wolff, D. B.: The TRMM Multi-satellite Precipitation Analysis: Quasi-Global,
 1874 Multi-Year, Combined-Sensor Precipitation Estimates at Fine Scale. *J. Hydrometeor.*, 8(1),
 1875 38-55, 2007.

1876 Josse, B., Simon P., and Peuch V-H.: Radon global simulations with the multiscale chemistry
 1877 and transport model MOCAGE, *Tellus B*, 56, 4, 339-356, 2004.

1878 Kelly, P. J., Kern C., Roberts T. J., Lopez T., Werner C., Aiuppa A.: Rapid chemical
 1879 evolution of tropospheric volcanic emissions from Redoubt Volcano, Alaska, based on
 1880 observations of ozone and halogen-containing gases, *Journal of Volcanology and Geothermal*
 1881 *Research*, 259, 317-333, 2013.

1882 Kern, C., Sihler H., Vogel L., Rivera C., Herrera M. and Platt U.: Halogen oxide
1883 measurements at Masaya Volcano, Nicaragua using active long path differential optical
1884 absorption spectroscopy, Bulletin of volcanology, 71, 6, 659-670, 2009.

1885 [Kern, C., T. Deutschmann, L. Vogel, M. Wöhrbach, T. Wagner, and U. Platt, Radiative](#)
1886 [transfer corrections for accurate spectroscopic measurements of volcanic gas emissions, Bull.](#)
1887 [Volcanol., 72, 233–247,doi:10.1007/s00445-009-0313-7, 2010.](#)

1888 [Kern, C., T. Deutschmann, C. Werner, A. J. Sutton, T. Elias, and P. J. Kelly, Improving the](#)
1889 [accuracy of SO2 column densities and emission rates obtained from upward-looking UV-](#)
1890 [spectroscopic measurements of volcanic plumes by taking realistic radiative transfer into](#)
1891 [account, J. Geophys. Res.,117, D20302, doi:10.1029/2012JD017936, 2012.](#)

1892 Kurosu, T. P., Chance K., and Sioris C. E.: Preliminary results for HCHO and BrO from the
1893 EOS-aura ozone monitoring instrument, In Fourth International Asia-Pacific Environmental
1894 Remote Sensing Symposium 2004: Remote Sensing of the Atmosphere, Ocean, Environment,
1895 and Space, pp. 116-123. International Society for Optics and Photonics, 2004.

1896 [Lee, C., Kim Y.-J., Tanimoto H., Bobrowski N., Platt U., Mori T., Yamamoto K., and Hong](#)
1897 [C.-S., High ClO and ozone depletion observed in the plume of Sakurajima volcano, Japan,](#)
1898 [Geophysical Research Letters, Geophys. Res. Lett., 32, 21, L21809,](#)
1899 [doi:10.1029/2005GL023785, 2005.](#)

1900 Lefèvre, J., Menkes, C., Bani, P., Marchesiello, P., Curci, G., Grell, G., ~~A., and~~ Frouin, R.:
1901 Distribution of sulfur aerosol precursors in the SPCZ released by continuous volcanic
1902 degassing at Ambrym, Vanuatu, ~~submitted to Journal of Volcanology and Geothermal~~
1903 ~~Research, J. Volcanol. Geoth. Res.,~~ doi:10.1016/j.jvolgeores.2015.07.018, in press 2015.

Mis en forme : Espace Avant : 6 pt,
Après : 0 pt

Mis en forme : author

Mis en forme : Citation HTML

Mis en forme : author

Mis en forme : author

Mis en forme : Citation HTML

Mis en forme : author

Mis en forme : Citation HTML

Mis en forme : author

Mis en forme : Citation HTML

Mis en forme : author

Mis en forme : Citation HTML

Mis en forme : author

Mis en forme : Citation HTML

Mis en forme : author

Mis en forme : Citation HTML

Mis en forme : author

Mis en forme : Citation HTML

Mis en forme : Citation HTML

Mis en forme : Citation HTML

Mis en forme : articletitle

Mis en forme : Citation HTML

Mis en forme : Citation HTML

Mis en forme : vol

Mis en forme : Citation HTML

Mis en forme : Citation HTML

Mis en forme : Citation HTML

1904 Li, C., J. Joiner, N. A. Krotkov, and Bhartia P. K., A fast and sensitive new satellite SO2
1905 retrieval algorithm based on principal component analysis: Application to the ozone
1906 monitoring instrument, *Geophys. Res. Lett.*, 40, 6314–6318, doi:10.1002/2013GL058134,
1907 2013.

1908 [Livesey, N.J., et al., 2011. Earth Observing System \(EOS\) Aura Microwave Limb Sounder](#)
1909 [\(MLS\) Version 3.3 and 3.4 Level 2 Data Quality and Description Document. Tech. Rep. JPL](#)
1910 [D-33509. NASA Jet Propulsion Laboratory, California Institute of Technology, Pasadena,](#)
1911 [California \(91109-8099, available at: <http://mls.jpl.nasa.gov/data/datadocs.php>\).](#)

1912 Logan, J. A., An analysis of ozonesonde data for the troposphere: Recommendations for
1913 testing 3-D models and development of a gridded climatology for tropospheric ozone, *J.*
1914 *Geophys. Res.*, 104(D13), 16,115–16,149, doi:10.1029/1998JD100096,1999.

1915 Longo, K. M., Freitas, S. R., Pirre, M., Marécal, V., Rodrigues, L. F., Panetta, J., Alonso, M.
1916 F., Rosário, N. E., Moreira, D. S., Gácita, M. S., Arteta, J., Fonseca, R., Stockler, R.,
1917 Katsurayama, D. M., Fazenda, A., and Bela, M.: The Chemistry CATT-BRAMS model
1918 (CCATT-BRAMS 4.5): a regional atmospheric model system for integrated air quality and
1919 weather forecasting and research, *Geosci. Model Dev.*, 6, 1389-1405, doi:10.5194/gmd-6-
1920 1389-2013, 2013.

1921 Marécal, V., Pirre M., Krysztofiak G., Hamer P. D., and Josse B.: what do we learn about
1922 bromoform transport and chemistry in deep convection from fine scale modelling?,
1923 *Atmospheric Chemistry and Physics*, 12, 14, 6073-6093, 2012.

1924 [Martin, R. S., Mather, T. A., and Pyle, D. M.: High-temperature mixtures of magmatic](#)
1925 [and atmospheric gases." *Geochemistry, Geophysics, Geosystems*, *Geochem. Geophys.*](#)
1926 [Geosyst.](#), 7, 4, Q04006, doi:10.1029/2005GC001186, 2006.

Mis en forme : Espace Avant : 6 pt,
Après : 0 pt

Mis en forme : author

Mis en forme : Citation HTML

Mis en forme : author

Mis en forme : Citation HTML

Mis en forme : Citation HTML

Mis en forme : Citation HTML

Mis en forme : author

Mis en forme : author

Mis en forme : Citation HTML

Mis en forme : articletitle

Mis en forme : articletitle

Mis en forme : Citation HTML

Mis en forme : vol

Mis en forme : Citation HTML

Mis en forme : Citation HTML

1927 Martin, R. S., Roberts T. J., Mather T. A., and Pyle D. M.: The implications of H₂S and H₂
 1928 kinetic stability in high-T mixtures of magmatic and atmospheric gases for the production of
 1929 oxidized trace species (eg, BrO and NO_x), *Chemical Geology*, 263, 1, 143-159, 2009.

1930 Martin, R. S., Ilyinskaya E., and Oppenheimer C.: The enigma of reactive nitrogen in
 1931 volcanic emissions, *Geochimica et Cosmochimica Acta*, 95, 93-105, 2012.

1932 Mather, T. A., A. G. Allen, C. Oppenheimer, D. M. Pyle, and A. J. S. McGonigle: Size-
 1933 resolved characterisation of soluble ions in the particles in the tropospheric plume of Masaya
 1934 volcano, Nicaragua: Origins and plume processing, *Journal of Atmospheric Chemistry* 46, 3,
 1935 207-237, 2003.

1936 Mather T.A, Pyle D.M, Allen A.G: Volcanic source for fixed nitrogen in the early Earth's
 1937 atmosphere. *Geology*. 32, 905–908, doi:10.1130/G20679.1, 2004.

1938 [Mosca, S.G.; Graziani, W.; Klug, R.; Bellasio; Bianconi R., “A statistical methodology for the](#)
 1939 [evaluation of long-range dispersion models: An application to the ETEX exercise.”, *Atmos.*](#)
 1940 [Environ.](#), 32, 4302–4324, 1998.

1941 Myhre, G., D. Shindell, F.-M. Bréon, W. Collins, J. Fuglestad, J. Huang, D. Koch, J.-F.
 1942 Lamarque, D. Lee, B. Mendoza, T. Nakajima, A. Robock, G. Stephens, T. Takemura and H.
 1943 Zhang, 2013: Anthropogenic and Natural Radiative Forcing. In: *Climate Change 2013: The*
 1944 *Physical Science Basis. Contribution of Working Group I to the Fifth Assessment Report of*
 1945 *the Intergovernmental Panel on Climate Change* [Stocker, T.F., D. Qin, G.-K. Plattner, M.
 1946 Tignor, S.K. Allen, J. Boschung, A. Nauels, Y. Xia, V. Bex and P.M. Midgley (eds.)].
 1947 Cambridge University Press, Cambridge, United Kingdom and New York, NY, USA.

1948 Naik, V., Voulgarakis, A., Fiore, A. M., Horowitz, L. W., Lamarque, J.-F., Lin, M., Prather,
 1949 M. J., Young, P. J., Bergmann, D., Cameron-Smith, P. J., Cionni, I., Collins, W. J., Dalsøren,

Mis en forme : Espace Avant : 6 pt,
Après : 0 pt

1950 S. B., Doherty, R., Eyring, V., Faluvegi, G., Folberth, G. A., Josse, B., Lee, Y. H.,
 1951 MacKenzie, I. A., Nagashima, T., van Noije, T. P. C., Plummer, D. A., Righi, M., Rumbold,
 1952 S. T., Skeie, R., Shindell, D. T., Stevenson, D. S., Strode, S., Sudo, K., Szopa, S., and Zeng,
 1953 G.: Preindustrial to present-day changes in tropospheric hydroxyl radical and methane
 1954 lifetime from the Atmospheric Chemistry and Climate Model Intercomparison Project
 1955 (ACCMIP), *Atmos. Chem. Phys.*, 13, 5277-5298, doi:10.5194/acp-13-5277-2013, 2013.

1956 Oppenheimer, C., Tsanev V. I., Braban C.F., Cox R. A., Adams J. W., Aiuppa A., Bobrowski
 1957 N., Delmelle P., Barclay J., McGonigle A.J. S.: BrO formation in volcanic plumes,
 1958 *Geochimica et Cosmochimica Acta*, 70, 12, 2935-2941, 2006.

1959 Oppenheimer, C., Kyle, P., Eisele, F., Crawford, J., Huey, G., Tanner, D., Kim, S., Maudlin,
 1960 L., Blake, D., Beyersdorf, A., Bub, M., and Davis, D.: Atmospheric chemistry of an
 1961 Antarctic volcanic plume, ~~*Journal of Geophysical Research: Atmospheres* (1984-2012)~~,
 1962 *Geophys. Res.*, 115, D4, D04303, doi:10.1029/2009JD011910, 2010.

1963 Popp C., McCormick B., Suleiman R., Chance K., Andrews B., Cottrell E.: Analysis of
 1964 volcanic bromine monoxide emissions in the southwestern Pacific region in 2005 based on
 1965 satellite observations from OMI, *Geophysical Research Abstracts* Vol. 17, EGU2015-9837,
 1966 2015.

1967 Putirka, K. D.: Thermometers and barometers for volcanic systems. In: Putirka, K. D. &
 1968 Tepley, F. (Eds.), *Minerals, Inclusions and Volcanic Processes*, *Reviews in Mineralogy and*
 1969 *Geochemistry* 69, 61–120, 2008.

1970 Prata, A.J., Carn, S.A., Stohl, A., Kerkmann, J., Long range transport and fate of a
 1971 stratospheric volcanic cloud from Soufrière Hills volcano, Montserrat. *Atmos. Chem.*
 1972 *Phys.* 7, 5093–5103, 2007.

Mis en forme : Espace Avant : 6 pt,
 Après : 0 pt, Ne pas ajuster l'espace
 entre le texte latin et asiatique, Ne pas
 ajuster l'espace entre le texte et les
 nombres asiatiques

Mis en forme : Citation HTML

Mis en forme : Citation HTML

Mis en forme : vol

Mis en forme : Citation HTML

Mis en forme : Citation HTML

Mis en forme : Espace Avant : 6 pt,
 Après : 0 pt

Mis en forme : Police :Times New
 Roman, 12 pt

1973 Pyle, D. M., and Mather T. A.: Halogens in igneous processes and their fluxes to the
1974 atmosphere and oceans from volcanic activity: a review." Chemical Geology, 263, 1, 110-
1975 121, 2009.

1976 [Remer, L.A., Kaufman, Y.J., Tanre, D., Mattoo, S., Chu, D.A., Martins, J.V., Li, R.R.,](#)
1977 [Ichoku, C., Levy, R.C., Kleidman, R.G., Eck, T.F., Vermote, E., Holben, B.N., The MODIS](#)
1978 [aerosol algorithm, products, and validation. J. Atmos. Sci. 62 \(4\), 947–973, 2005.](#)

1979 [Remer, L.A., Kleidman R. G., Levey R.C., Kaufmann Y.J., Tanré D., Mattoo S., Martins J.V.,](#)
1980 [Ichoku C., Koren I., Yu H., Holben B.N., Global aerosol climatology from the MODIS](#)
1981 [satellite sensors, J. Geophys. Res., 113, D14S07, doi:10.1029/2007JD009661, 2008.](#)

1982 Roberts, T. J., Braban C. F., Martin R. S., Oppenheimer C., Adams J. W., Cox R. A., Jones R.
1983 L., and Griffiths P. T.: Modelling reactive halogen formation and ozone depletion in volcanic
1984 plumes, Chemical Geology, 263, 1, 151-163, 2009.

1985 Roberts, T. J., Martin, R. S. and Jourdain L.: Reactive bromine chemistry in Mount Etna's
1986 volcanic plume: the influence of total Br, high-temperature processing, aerosol loading and
1987 plume–air mixing, Atmospheric Chemistry and Physics, 14, 20, 11201-11219, 2014a.

1988 Roberts, T. J., Jourdain L., Griffiths P. T., and Pirre M., Re-evaluating the reactive uptake of
1989 HOBr in the troposphere with implications for the marine boundary layer and volcanic
1990 plumes, Atmospheric Chemistry and Physics, 14, 20, 11185-11199, 2014b.

1991 Roberts T. J., Vignelles D., Liuzzo M., Giudice G., Aiuppa A., Chartier M., Coute B., Lurton
1992 T., Berthet G., Renard J.-B., Advances in in-situ real-time monitoring of volcanic emissions:
1993 HCl, and size-resolved aerosol at Mt Etna (passive degassing), submitted to Geochimica et
1994 Cosmochimica Acta, 2015.

Mis en forme : Espace Avant : 6 pt,
Après : 0 pt

Mis en forme : Espace Avant : 6 pt,
Après : 0 pt

1995 Robin, C., Eissen, J.-P. and Monzier, M.: Giant tuff cone and 12-km-wide associated caldera
 1996 at Ambrym Volcano (Vanuatu, New Hebrides Arc). J. Volcanol. Geotherm. Res., 55: 225-
 1997 238, 1993.

1998 Roine A. (2007). HSC ~~chemistry~~ Chemistry 6.1. Tech. rep. Outotec Research Oy, Pori,
 1999 Finland, 2007.

2000 Rosário, N. E., Longo K. M., Freitas S. R., Yamasoe M. A., and Fonseca R. M.: Modeling the
 2001 South American regional smoke plume: aerosol optical depth variability and surface
 2002 shortwave flux perturbation, Atmos. Chem. Phys, 13, 2923-2938, 2013.

2003 Rotstajn, L. D., and U. Lohmann, Simulation of the tropospheric sulfur cycle in a global
 2004 model with a physically based cloud scheme, J. Geophys. Res., 107(D21), 4592,
 2005 doi:10.1029/2002JD002128, 2002.

2006 Saiz-Lopez, A., J. M. C. Plane, and J. A. Shillito : Bromine oxide in the mid-latitude
 2007 marine boundary layer, Geophys. Res. Lett., 31, L03111, doi:10.1029/2003GL018956, 2004.

2008 ~~Sander, S. P., et al. Chemical kinetics and photochemical data for use in atmospheric studies:~~
 2009 ~~evaluation number 15. Pasadena, CA: National Aeronautics and Space Administration, Jet~~
 2010 ~~Propulsion Laboratory, California Institute of Technology, 2006.~~

2011 ~~Sander, R.:~~ Compilation of Henry's Law Constants for Inorganic and Organic Species of
 2012 Potential Importance in Environmental Chemistry, ~~1999 (www.henry's-law.org) available at:~~
 2013 <http://www.henrys-law.org/henry-3.0.pdf> (last access: November 2015), 1999.

2014 [Sander, S. P., Friedl, R. R., Golden, D. M., Kurylo, M. J., Moortgat, G. K., Keller-Rudek, H.,](#)
 2015 [Wine, P. H., Ravishankara, A. R., Kolb, C. E., Molina, M. J., Finlayson-Pitts, B. J., Huie, R.](#)
 2016 [E., and Orkin, V. L.: Chemical Kinetics and Photochemical Data for Use in Atmospheric](#)
 2017 [Studies, Evaluation Number 15, JPL Publication 06-2, Jet Propulsion Laboratory, Pasadena,](#)

Mis en forme : Couleur de police :
Noir, Anglais (États Unis)

Mis en forme : Anglais (États Unis)

Mis en forme : Couleur de police :
Noir

Mis en forme : Espace Avant : 6 pt,
Après : 0 pt, Ne pas ajuster l'espace
entre le texte latin et asiatique, Ne pas
ajuster l'espace entre le texte et les
nombres asiatiques

2018 [CA, available at http://jpldataeval.jpl.nasa.gov/pdf/JPL_15_AllInOne.pdf](http://jpldataeval.jpl.nasa.gov/pdf/JPL_15_AllInOne.pdf) (last access:
2019 [November 2015](#)), 2006.

2020 Schmidt, A., Carslaw K. S., Mann G. W., Wilson M., Breider T. J., Pickering S. J., and
2021 Thordarson T: The impact of the 1783–1784 AD Laki eruption on global aerosol formation
2022 processes and cloud condensation nuclei. *Atmospheric Chemistry and Physics* 10, 13, 6025-
2023 6041, 2010.

2024 Schmidt, A., Carslaw K. S., Mann G. W., Rap A., Pringle K. J., Spracklen D. V., Wilson M.,
2025 and Forster P. M.: Importance of tropospheric volcanic aerosol for indirect radiative forcing
2026 of climate, *Atmospheric Chemistry and Physics*, 12, 16, 7321-7339, 2012.

2027 Simpson, W. R., Brown S. S., Saiz-Lopez A., Thornton J. A., and von Glasow R.:
2028 Tropospheric Halogen Chemistry: Sources, Cycling, and Impacts, *Chemical reviews*, 2015.

2029 Schultz, M., Backman, L., Balkanski, Y., Bjoernsdalsaeter, S., Brand, R., Burrows, J.,
2030 Dalsoeren, S., de Vasconcelos, M., Grodtmann, B., Hauglustaine, D., Heil, A., Hoelzemann,
2031 J., Isaksen, I., Kaurola, J., Knorr, W., Ladstaetter-Weienmayer, A., Mota, B., Oom, D.,
2032 Pacyna, J., Panasiuk, D., Pereira, J., Pulles, T., Pyle, J., Rast, S., Richter, A., Savage, N.,
2033 Schnadt, C., Schulz, M., Spessa, A., Staehelin, J., Sundet, J., Szopa, S., Thonicke, K., van het
2034 Bolscher, M., van Noije, T., van Velthoven, P., Vik, A., and Wittrock, F.: REanalysis of the
2035 TROpospheric chemical composition over the past 40 years (RETRO). A long-term global
2036 modeling study of tropospheric chemistry. Final Report, Tech. rep., Max Planck Institute for
2037 Meteorology, Hamburg, Germany, 2007.

2038 Schumann, U., Weinzierl, B., Reitebuch, O., Schlager, H., Minikin, A., Forster, C., Baumann,
2039 R., Sailer, T., Graf, K., Mannstein, H., Voigt, C., Rahm, S., Simmet, R., Scheibe, M.,
2040 Lichtenstern, M., Stock, P., Rüba, H., Schauble, D., Tafferner, A., Rautenhaus, M., Gerz, T.,
2041 Ziereis, H., Krautstrunk, M., Mallaun, C., Gayet, J.-F., Lieke, K., Kandler, K., Ebert, M.,

Mis en forme : Espace Avant : 6 pt,
Après : 0 pt

2042 Weinbruch, S., Stohl, A., Gasteiger, J., Groß, S., Freudenthaler, V., Wiegner, M., Ansmann,
2043 A., Tesche, M., Olafsson, H., and Sturm, K.: Airborne observations of the Eyjafjalla volcano
2044 ash cloud over Europe during air space closure in April and May 2010, Atmos. Chem. Phys.,
2045 11, 2245-2279, doi:10.5194/acp-11-2245-2011, 2011.

2046 Seinfeld, J. H., and A. N. Pandis, A. N.: Properties of the atmospheric aerosol, in:
2047 Atmospheric chemistryChemistry, and physicsPhysics – from air pollutionAir Pollution to
2048 climate changeClimate Change, Chapter 8, John Wiley and Sons, Chapter 8 Properties of the
2049 Atmospheric Aerosol, pagesNew Jersey, United States of America, 350–394, 2006.

2050 Simkin, T., and Siebert, L.: Global Volcanism FAQs, Smithsonian Institution, Global
2051 Volcanism Program Digital Information Series, GVP 5, available at:
2052 <http://www.volcano.si.edu/education/questions/> (last access: August 2010), 2002.

2053 Siebert, L., Simkin, T., and Kimberly, P.: Volcanoes of the World, 3rd ed. Berkeley:
2054 University of California Press, United States of America, 568 p, 2010.

2055 Sheehan, F. and Barclay, J.: Staged storage and magma recycling at Ambrym volcano,
2056 Vanuatu, submitted to JVGRI. Volcanol. Geoth. Res., doi:10.1016/j.jvolgeores.2016.02.024,
2057 in press 2016.

2058 Simpson, W. R., Brown, S. S., Saiz-Lopez, A., Thornton, J. A., and von Glasow, R.:
2059 Tropospheric halogen chemistry: sources, cycling, and impacts, Chem. Rev., 115 (10), pp
2060 4035–4062, doi: 10.1021/cr5006638, 2015.

2061 Stevenson, D. S., Johnson C. E., Collins W. J., and Derwent R. G.: The tropospheric sulphur
2062 cycle and the role of volcanic SO₂, Geological Society, London, Special Publications 213, 1,
2063 295-305, 2003.

Mis en forme : Couleur de police :
Noir

Mis en forme : Couleur de police :
Noir

Mis en forme : Couleur de police :
Noir

Mis en forme : Couleur de police :
Noir

Mis en forme : Couleur de police :
Noir

Mis en forme : Couleur de police :
Noir

Mis en forme : Couleur de police :
Noir

Mis en forme : Couleur de police :
Noir

Mis en forme : Couleur de police :
Noir

Mis en forme : Couleur de police :
Noir

Mis en forme : Couleur de police :
Noir

Mis en forme : Couleur de police :
Noir

Mis en forme : Couleur de police :
Noir

Mis en forme : Espace Avant : 6 pt,
Après : 0 pt

2064 Stockwell, W. R., Kirchner F., Kuhn M. and Seefeld S.: A new mechanism for regional
2065 atmospheric chemistry modeling, Journal of Geophysical Research: Atmospheres (1984–
2066 2012), 102, D22, 25847-25879, 1997.

2067 Surl, L., Donohoue D., Aiuppa A., Bobrowski N., and von Glasow R.: Quantification of the
2068 depletion of ozone in the plume of Mount Etna, Atmospheric Chemistry and Physics 15, 5
2069 2613-2628, 2015.

2070 Tabazadeh, A., Toon O. B., Clegg S. L., Hamill P.: A new parameterization of H2SO4/H2O
2071 aerosol composition: Atmospheric implications, Geophysical Research Letters, 24, 15, 1931-
2072 1934, 1997.

2073 Theys, N., ~~M.~~ Van Roozendael ~~M.~~, ~~B.~~ Dils ~~B.~~, ~~F.~~ Hendrick ~~F.~~, ~~N.~~ Hao ~~N.~~, and De
2074 ~~Maziere~~ Mazière M.: First satellite detection of volcanic bromine monoxide emission after
2075 the Kasatochi eruption, ~~Geophysical Research Letters~~, Geophys. Res. Lett., 36, ~~3~~, L03809,
2076 doi:10.1029/2008GL036552, 2009.

2077 Theys, N., De Smedt, I., Van Roozendael, M., Froidevaux, L., Clarisse, L., Hendrick, F.,
2078 First satellite detection of volcanic OClO after the eruption of Puyehue-Cordón Caulle.
2079 Geophys. Res. Lett. 41, 667–672. http://dx.doi.org/10.1002/2013GL058416, 2014.

2080 Tie, X., S. Madronich, S., Walters S., R. Zhang R., P. Rasch P., and Collins W. Effect of
2081 clouds on photolysis and oxidants in the troposphere, Journal of Geophysical Research:
2082 Atmospheres (1984–2012), J. Geophys. Res., 108, ~~D20~~, 4642, doi:10.1029/2003JD003659,
2083 2003.

2084 Vance, A., A. J. S. McGonigle, A. J. S., Aiuppa A., J. L., Stith J. L., K. Turnbull K., and
2085 von Glasow R. Ozone depletion in tropospheric volcanic plumes, Geophysical Research
2086 Letters, Geophys. Res. Lett., 37, ~~22~~, L22802, doi:10.1029/2010GL044997, 2010.

- Mis en forme : auteur
- Mis en forme : Espace Avant : 6 pt. Après : 0 pt, Ne pas ajuster l'espace entre le texte latin et asiatique, Ne pas ajuster l'espace entre le texte et les nombres asiatiques
- Mis en forme : Citation HTML
- Mis en forme : auteur
- Mis en forme : Citation HTML
- Mis en forme : auteur
- Mis en forme : auteur
- Mis en forme : auteur
- Mis en forme : auteur
- Mis en forme : Citation HTML
- Mis en forme : auteur
- Mis en forme : Citation HTML
- Mis en forme : Citation HTML
- Mis en forme : articletitle
- Mis en forme : Citation HTML
- Mis en forme : Citation HTML
- Mis en forme : vol
- Mis en forme : Citation HTML
- Mis en forme : Citation HTML
- Mis en forme : auteur
- Mis en forme : Citation HTML
- Mis en forme : auteur
- Mis en forme : auteur
- Mis en forme : auteur
- Mis en forme : auteur
- Mis en forme : Citation HTML
- Mis en forme : Citation HTML
- Mis en forme : articletitle
- Mis en forme : Citation HTML
- Mis en forme : Citation HTML
- Mis en forme : vol
- Mis en forme : Citation HTML
- Mis en forme : Citation HTML

2087 van der Werf, G. R., Randerson J. T., Giglio L., Collatz G. J., Kasibhatla P. S. and Arellano
2088 Jr, A. F.: Interannual variability in global biomass burning emissions from 1997 to 2004,
2089 Atmospheric Chemistry and Physics, 6, 11, 3423-3441, 2006.

2090 Voigt, C., P. Jessberger, T. Jurkat, S. Kaufmann, R. Baumann, H. Schlager, N. Bobrowski, G.
2091 Giuffrida, and G. Salerno: Evolution of CO₂, SO₂, HCl, and HNO₃ in the volcanic plumes
2092 from Etna, Geophysical Research Letters, 41, 6, 2196-2203, 2014.

2093 von Glasow, R., Bobrowski N., and Kern C.: The effects of volcanic eruptions on atmospheric
2094 chemistry, Chemical Geology, 263, 1, 131-142, 2009.

2095 von Glasow, R.: Atmospheric chemistry in volcanic plumes, Proceedings of the National
2096 Academy of Sciences, 107, 15, 6594-6599, 2010.

2097 Walko, R. L., Band L. E., Baron J., Kittel T. G. F., Lammers R., Lee T. J., Ojima D., Pielke
2098 Sr R. A., Tayloer C., Tague C., Tremback C. J., Vidale P.L: Coupled atmosphere-biophysics-
2099 hydrology models for environmental modeling. Journal of applied meteorology, 39, 6, 931-
2100 944, 2000.

2101 Wang T. X., Kelley M. D., Cooper J. N., Beckwith R. C., and Margerum D. W.: Equilibrium,
2102 kinetic, and UV-spectral characteristics of aqueous bromine chloride, bromine, and chlorine
2103 species, Inorganic Chemistry, 33, 25, 5872-5878, 1994.

Mis en forme : Espace Avant : 6 pt,
Après : 0 pt

2104
2105
2106
2107
2108
2109
2110

Mis en forme : Gauche, Espace Avant
: 0 pt, Ne pas ajuster l'espace entre le
texte latin et asiatique, Ne pas ajuster
l'espace entre le texte et les nombres
asiatiques

2111 **Tables:**

2112

Reaction	Reactive uptake coefficient
$HOBr + H^+_{(aq)} + Br^-_{(aq)} \rightarrow Br_{2(aq \rightarrow g)} + H_2O$ <u>$HOBr + H^+_{(aq)} + Br^-_{(aq)} \rightarrow Br_{2(aq \rightarrow g)} + H_2O$</u>	$0.2 \times \frac{[Br_{2(aq)}]}{[Br_{2(aq)}] + [BrCl_{(aq)}]}$ <u>$0.2 \times \frac{[Br_{2(aq)}]}{[Br_{2(aq)}] + [BrCl_{(aq)}]}$</u>
$HOBr + H^+_{(aq)} + Cl^-_{(aq)} \rightarrow BrCl_{(aq \rightarrow g)} + H_2O$ <u>$HOBr + H^+_{(aq)} + Cl^-_{(aq)} \rightarrow BrCl_{(aq \rightarrow g)} + H_2O$</u>	$0.2 \times \frac{[BrCl_{(aq)}]}{[Br_{2(aq)}] + [BrCl_{(aq)}]}$ <u>$0.2 \times \frac{[BrCl_{(aq)}]}{[Br_{2(aq)}] + [BrCl_{(aq)}]}$</u>
$BrONO_2 + H_2O \rightarrow HOBr_{(aq \rightarrow g)} + HNO_3$ <u>$BrONO_2 + H_2O \rightarrow HOBr_{(aq \rightarrow g)} + HNO_3$</u>	0.8

2113

2114

2115 **Table 1:** Heterogeneous reactions in the model and their associated reactive uptake
2116 coefficients on sulfate aerosol. See section 2.3.1 for description of the calculation of the ratio

2117
$$\frac{[BrCl_{(aq)}]}{[Br_{2(aq)}] + [BrCl_{(aq)}]} \frac{[Br_{2(aq)}]}{[Br_{2(aq)}]}.$$

Code de champ modifié

2118

2119

2120

2121

2122

2123

2124
2125
2126
2127
2128
2129
2130
2131

Mis en forme : Police :Non Gras

Volcano	Reported activity	Emission (kt/day)	Source	
Gaua	None	0,070 kt/day	AEROCOM database (a)	2132 2133 2134
Aoba (Ambae)	None	0.070 kt/day	AEROCOM database (b)	2135 2136
Ambrym	Extreme passive degassing	18.835 kt/day	Bani et al. (2012) (c)	2137 2138 2139
Lopevi	Not clear	0.070 kt/day	Bani et al. (2012) (d)	2140
Epi	None	0.070 kt/day	AEROCOM database (e)	2141
Yasur	Eruption	0.968 kt/day	Bani et al. (2012) (f)	2142

2143

2144 **Table 2:** SO₂ emission rates in January 2005 from the principal active Vanuatu’s volcanoes (
2145 Gaua, Aoba, Lopevi, Epi, Ambrym, Yasur) as prescribed in the simulations. Details for each
2146 volcano are given in the following:

- a) In Bani et al. (2012), only information during a phase of eruptive activity. We prescribed the post eruptive degassing rate (for the volcanoes that had an eruption since 1900) of 0.070 kt/day assigned for this volcano in the AEROCOM database.
- b) Before eruption of nov. 2005, no significant passive degassing. We prescribed the post eruptive degassing rate of 0.070 kt/day assigned in the AEROCOM database.
- c) Mean of 5 transverses of 12 January 2005 in Bani et al. (2012). Note that, in the fourth grid, the two Marum and Benbow cones do not lie in the same gridbox. As a result, we prescribed 60% of the emission in the model gridbox containing Marum and 40% in the gridbox containing Benbow as found in Bani et al. (2009). Note, that in the AEROCOM database, the value is 0.0807kt/day.
- d) Lopevi is a volcano with frequent degassing. From Bani et al. (2006), vapor was observed covering the crater but it was difficult to conclude on its volcanic activity. Local observers in Vanuatu indicated ongoing eruptive activity at Lopevi starting at the end of January 2005 and continuing on February (GPV). Mean of 3 traverses of passive degassing of 24/02/2006 was 0.156 kt/day. As a result, we kept the value of AEROCOM database of 0.070 kt/day.
- e) No information. Post eruptive degassing rate of 0.070 kt/day is assigned in AEROCOM database.
- f) Value of 10/01/05 of Bani et al. (2012). In AEROCOM database, it is 0.900 kt/day

2171
2172
2173
2174
2175
2176
2177
2178
2179

Gas	MixingMass mixing ratio in HSC input
H ₂ O	9.29 E-01
N ₂	1.56E-02
CO ₂	3.80E-02
SO ₂	1.05E-02
HCl	1.84E-03
O ₂	4.20E-03
Ar	2.00E-04
HBr	7.23E-06
HF	7.53E-04

Tableau mis en forme

2180

2181 **Table 3:** Composition inputs to the HSC Chemistry model assuming plume-air mixture of
2182 98:2 magmatic:atmospheric gases, with temperatures 1125 °C and 20 °C, resulting in mixed

2183 temperature of 1103 °C. Resulting output of the HSC Chemistry simulations were converted
 2184 to ratios relative to sulfur and used to initialize the S1_HighT model simulation (second row
 2185 of Table 4). The HSC Chemistry model is presented in section 2.3.3-4.

2186

2187

2188

2189

2190

2191

2192

Simulations	HCl/SO ₂	HBr/SO ₂	H ₂ SO ₄ /SO ₂	Cl/SO ₂	Br/SO ₂	OH/SO ₂	NO/SO ₂
S1	0.1	8.75e-04	1.55e-02	0	0	0	0
S1_HighT	0.1	6.87e-04	1.55e-02	1.33e-04	1.89e-04	7.04e-04	7.45e-04
S1_HighT_noN Ox	0.1	6.87e-04	1.55e-02	1.33e-04	1.89e-04	7.04e-04	0
S1_no_hal Ambrym only	0	0	0	0	0	0	0
S1_no_hal2 Ambrym only	0	0	0	0	0	7.04e-04	0
S0 Ambrym only	0	0	0	0	0	0	0

2193
2194
2195
2196
2197
2198
2199
2200
2201
2202
2203
2204
2205
2206
2207
2208
2209
2210
2211
2212

Table 4: Emissions of HCl, HBr, sulfate and radicals (Cl, Br, OH, NO) expressed in terms of mass ratios relative to SO₂ emissions for all the volcanoes within the domain study and for the different simulations (see section 2.3.3 for the details on the ratios derivation and section 2.3.4 for details on the simulations). Note that for S1_no_hal, S1_no_hal2 and S0 simulations, the ratios indicated here are only for the emissions of the Ambrym volcano. These simulations have the same emissions than S1_HighT except for Ambrym volcano whose emission in these simulations is indicated in the table other volcanoes within the domain study. Note also that all the simulations, except S0, have an ~~emission of~~ SO₂ emission for Ambrym of 18.8 kt/day ~~and a sulfate aerosol emission (1% of sulfur (=SO₂+H₂SO₄)).~~ S0 does not include any volcanic emissions from Ambrym.

	Mean SO ₂	Mean BrO	r _{SO2}	r _{BrO}	RMSE _{SO2}	RMSE _{BrO}
DOAS	2.29 e18	5.84 e14				
S1	2.27 e18	1.14 e14	0.62	-0.21	1.09e18	5.97e14
S1_HighT	2.25e18	3.42e14	0.61	0.59	1.10e18	3.90e14

2213 **Table 5:** Statistical comparison between [the](#) DOAS SO₂ and BrO columns [from the 5](#)
2214 [traverses of the Ambrym plume on 12 th January 2005](#) and the corresponding simulated
2215 values (for S1 and S1_HighT). Correlation coefficients (r), root mean square error (RMSE in
2216 molecule. cm⁻²) are given as well as mean values (molecule. cm⁻²) of observed and
2217 simulated data. Note that we did not include here the data for which we did not have GPS data
2218 (dashed lines of Figures 3 and 4).

2219
2220
2221
2222
2223
2224
2225
2226
2227
2228
2229
2230
2231
2232

2233 **Figure captions:**

2234 **Figure 1:** Vertical distribution of volcanic emissions from Ambrym as prescribed in the
2235 model for the all the simulations (black line) except for the sensitivity simulations
2236 S1_HighT_alt (blue line), S1_HighT_width (orange line). See section 2.3.4 for details on
2237 simulations.

2238 **Figure 2:** a) Top: Position of the nested model grids (blue lines) and of the volcanoes (red
2239 filled circles) taken into account in the simulations. For clarity, only the 3 largest model grids
2240 are shown. b) Bottom: Zoom on the two smallest model grids (blue lines) and on the
2241 volcanoes (red filled circles) taken into account in the simulations. Resolution of each grid is
2242 given in section 2.3.4.

2243 **Figure 3:** Comparison between SO₂ columns observed by Bani et al. (2009) (red line) and
2244 simulated by the model for S1 (black line), S1_HighT (blue line). Each panel represents a
2245 traverse of the Ambrym plume in the cross-wind direction on the 12 th January 2005 between
2246 05:00 UT and 06:00 UT, at a range of distances downwind. [The traverse at 21 km from the](#)
2247 [source is not shown here but is included in Table 5.](#) The x-axis shows the datapoint number in
2248 the transect across the plume (Bani et al., 2009). The direction of each transect across the
2249 plume has a east-west component. Here, each transect is shown with the datapoints from
2250 west to east (left to right). Note that model results are for the same position and time as the
2251 measurements and for the finest grid (0.5 km x0.5 km) except when GPS data (longitude and
2252 latitude) were not available. In this case, model results (dashed lines) were interpolated
2253 between the last and the next positions for which we had GPS data. Note that black and blue
2254 lines are on top of each other (superimposed). Reported error from DOAS measurements (1σ)
2255 is 2.45×10^{16} molec./cm²

2256

Figure 4: Comparison between BrO columns observed by Bani et al. (2009) (red line) and simulated by the model for S1 (black line), S1_HighT (blue line). See Figure 3 for details on the method of comparison. Reported error (1 σ) is 1.22×10^{14} molec./cm².

Figure 5: Variation of BrO/SO₂ ratios with distance from the vent derived from observations (top) and model simulations S1 (middle), S1_HighT (bottom) presented in Figure 3 and 4. For each transect, each BrO/SO₂ ratio has been colored according to its SO₂ column value relative to the maximal value of the SO₂ column (SO₂_max) for this transect. More precisely, the

color indicates the relative difference $\frac{(SO_2_max - SO_2)}{SO_2_max}$. Note that we did

Code de champ modifié

not include the observations nor the corresponding model results for which we did not have GPS data (dashed lines of Figures 3 and 4).

Figure 6: Distance-Pressure cross section of the SO₂, OH, HBr, BrO, O₃ and NO_x mixing ratios in the plume of Ambrym on 12th January 2005 at 06 UT in the simulation S1.

Figure 7: Br speciation along the plume (in the core and at the edge) in the simulation S1 and the grid 2 km x 2 km the 12th of January 2005 at 06 UT. The Br speciation has been calculated as the percent of Bry (Bry= HBr + 2Br₂ + BrCl+ Br + BrO + HOBr + BrONO₂). Distance is calculated from the middle of the gridbox containing Marum and Benbow.

Figure 8: Distance-Pressure cross section of the SO₂, OH, HBr, BrO, O₃ and NO_x mixing ratios in the plume of Ambrym on 12th January 2005 at 06 UT in the simulation S1_HighT.

Figure 9: Br speciation along the plume (in the core and at the edge) in the simulation S1_HighT and the grid 2 km x 2 km the 12th of January 2005 at 06 UT. The Br speciation has been calculated as the percent of Bry (Bry= HBr + 2Br₂ + BrCl+ Br + BrO + HOBr + BrONO₂). Distance is calculated from the middle of the gridbox containing Marum and Benbow.

2280 **Figure 10:** Top: OMI SO₂ columns (1×10^{16} molecule/cm²) for the 12th January 2005 at 02 :
2281 30 UT. Bottom: Simulated SO₂ columns (1×10^{16} molecule/cm²) (S1_HighT) from the grid
2282 10km x 10km for the 12th January 2005 at 03:00 UT interpolated onto the OMI grid.

2283 **Figure 11:** Daily mean difference (12th January 2005) between simulated sulfate in
2284 S1_HighT and S0 at 875 hPa, 500 hPa and 150 hPa for the grid 50 km x 50 km.

2285 **Figure 12:** Profile of the daily (12th January 2005) mean mixing ratios (pptv) of sulfate
2286 simulated by the model in the larger grid (of resolution 50 km x 50 km) in S1_HighT (black)
2287 and in S0 (light blue).

2288 **Figure 13:** Daily precipitation (mm/day) for the 12th January 2005 as estimated from the
2289 TRMM satellite (3B42 product) and simulated by the model.

2290 **Figure 14:** Fifteen-days forward trajectories initialized from the location of Ambrym volcano
2291 at 1373 m every hour on the 10th and 11th January 2005 calculated with the HYSPLIT model.
2292 The color scale represents the pressure (in hPa) of the air masses along the trajectories.

2293 **Figure 15:** Daily mean difference (12th January 2005) between simulated Br_y (pptv) in
2294 S1_HighT and in S0 at 875 hPa, 500 hPa, 150 hPa and 80 hPa for the 50 km x 50 km grid.

2295 **Figure 16:** Left: Profile of the daily (12th January 2005) mean mixing ratios of Br_y simulated
2296 by the model in the larger grid (50 km x 50 km) in S1_HighT (black) and in S0 (light blue).
2297 Right: Daily mean (12th January 2005) of the Br speciation (%) for the simulation S1_HighT
2298 for grid boxes where Br_y mean difference between S1_HighT and S0 is larger than 0.5 pptv
2299 (Figure 15).

2300 **Figure 17:** Daily mean difference (12th January 2005) between simulated ozone (~~(%)~~) in
2301 S1_HighT and in S0 (in % relative to S0) at 875 hPa, 500 hPa for the 50 km x 50 km grid.

2302